MECHANICAL AND FRACTURE PROPERTIES OF PUMICE LIGHTWEIGHT AGGREGATE STEEL FIBER REINFORCED CONCRETE

by
Ali Can Epözdemir
B.S., Civil Engineering, Istanbul Technical University 2014

Submitted to the Institute for Graduate Studies in
Science and Engineering in partial fulfillment of
requirement for the degree of
Master of Science

Graduate Program in Civil Engineering
Boğaziçi University
2019

ACKNOWLEDGEMENTS

First of all, I am very much obliged to my advisor Prof. Turan Özturan for his contributions throughout the thesis and my graduate studies. I have learned a lot from his guidance and understanding, not only concerning engineering but also about life itself.

I would like to express my gratitude to Prof. Stratis Badoginannis for his mentoring and guidance for the thesis. His great support made this thesis possible.

I would like to thank Assoc. Prof. Nilüfer Özyurt Zihnioğlu for her valuable suggestions to give the thesis its last shape. Also I am very grateful to Asist. Prof. Zeynep Başaran, for her comments and participation in the jury.

I would like to thank Grigoris, Kostas and other Greek friends who helped me a lot for the experimental part of the thesis.

Finally, I am thankful to my family and especially to my lovely sister Naz for their never-ending support.

ABSTRACT

MECHANICAL AND FRACTURE PROPERTIES OF PUMICE-LIGHTWEIGHT AGGREGATE STEEL FIBER REINFORCED CONCRETE

Composite materials are widely used with many purposes in contemporary engineering applications. Lightweight composites are mostly used in aerospace and military engineering applications but as well as in construction industry. Reducing the dead loads of the structures has numerous advantages. For this purpose there are several different lightweight aggregates used in the literature. In the context of the current study pumice type of lightweight aggregates used with normal weight aggregates. Steel fibers with different aspect ratios (55, 57 and 65) having the length 30mm, 36mm and 60mm respectively used with two different volume fractions of 0.5% and 1%.Fresh state properties as well as hardened state properties are investigated. Several mechanical properties such as compressive strength, indirect tensile strength, modulus of elasticity etc. are presented. Three different type of fracture tests conducted; namely 3 point bending test with notched specimens, Barcelona test and Generalized Barcelona test. Effect of fiber addition, fiber volume fraction and aspect ratio are investigated evaluating toughness of specimens. Considering Barcelona tests both total circumferential opening displacement (TCOD) and axial displacements used to evaluate the ductile behavior of concrete. Finally, it was observed that increase in fiber volume fraction and aspect ratio significantly improves mechanical and fracture properties of pumice lightweight aggregate concrete.

ÖZET

PONZA (PUMICE) HAFİF AGREGALI ÇELİK LİFLİ BETONUN MEKANİK VE KIRILMA ÖZELİKLERİ

Günümüz mühendislik uygulamalarında kompozit malzemeler birçok farklı amaçla kullanılıyor. Hafif kompozit malzemeler çoğunlukla havacılık ve askeri mühendislik alanlarında kullanılmakla beraber yapı sanayiinde de kullanılıyor. Yapının ölü yükünü hafifletmenin birçok avantajı var. Bu amaçla, literatürde farklı türde hafif agregaların kullanıldığı çalışmalar bulunuyor. Mevcut tez çalışması kapsamında ponza (pumice) tipi hafif agregalar normal ağırlıktaki agregalarla birlikte kullanılmıştır. Farklı narinlik oranlarında (55, 57 ve 65) ve 30mm, 36mm ve 60mm boylarında üç tip çelik lif %0.5 ve 1% hacim oranlarında kullanılmıştır. Akışkan ve katı haldeki beton özellikleri incelenmiştir. Basınç dayanımı, dolaylı çekme dayanımı, Elastisite modülü gibi bazı mekanik özellikler sunulmuştur. 3 farklı tipte kırılma deneyi uygulanmıştır: 3 noktalı eğilme deneyi, Barcelona ve Genelleştirilmiş Barcelona deneyleri. Lif eklemenin, lif hacim ve narinlik oranının etkileri tokluk davranışı üzerinden incelenmiştir. Barcelona testi kapsamında hem toplam çevresel açılma deplasmanı hem de eksenel deplasmanlar betonun sünek davranışı açısından araştırılmıştır. Sonuç olarak, çelik lif hacim ve narinlik oranının artırılmasının betonun mekanik ve kırılma davranışlarını geliştirdiği gözlemlenmiştir.

TABLE OF CONTENTS

ACKNOWLEDGEMENTS iii
ABSTRACT iv
ÖZET v
LIST OF FIGURES ix
LIST OF TABLES xii
LIST OF SYMBOLS xiv
LIST OF ACRONYMS/ABBREVIATIONS xvi
1. INTRODUCTION 1
2. LITERATURE REVIEW 3
2.1. Composite Materials 3
2.1.1. Fiber Reinforcement 5
2.1.2. Matrix 6
2. 1. 3. Matrix – Fiber Interface 7
2.1.3.1. Pre-cracked stress transfer 10
2.1.3.2 Post-crack stress transfer 11
2.2. Steel fiber usage in composite materials 12
2.2.1. Fiber orientation and distribution 14
2.2.2. Workability 16
2.2.3. Effect on Mechanical Properties 18
2.3. Lightweight Aggregates in Composite Materials 20
2.3.1. Lightweight Aggregate Concrete (LWAC) 20
2.3.2. Fresh State Properties of LWAC 22
2.3.3. Mechanical Properties of LWAC 23
2.4. Pumice Lightweight Aggregate Steel Fiber-Reinforced Concrete 25
2.4.1. Compressive Strength and Elastic Modulus of Pumice LWASFRC 26
2.4.2. Tensile Strength of Pumice LWASFRC 27

2.4.3. Flexural Strength and Behavior of Pumice LWASFRC....27
3. MATERIALS AND METHODS....29
3.1. Materials....29
3.1.1. Cement....29
3.1.2. Silica Fume....29
3.1.3. Aggregates....31
3.1.4. Fibers....31
3.1.5. Superplasticizer....32
3.2. Mix Proportions and Casting....32
3.2.1. Aggregate Grading....32
3.2.2. Mixture Design....34
3.3. Casting and Specimens' Preparation....35
3.3.1. Specimens' Preparation....35
3.3.2. Capping....37
3.3.3. Preparation of Barcelona Test Specimens....38
3.4. Testing Machines....39
3.5. Testing Procedures....39
3.5.1 Tests and Calculations for Fresh State Properties....39
3.5.1.1. Slump Test....39
3.5.1.2. Density Test and Air Content Measurement....39
3.5.2. Tests for Hardened State Properties....40
3.5.2.1. Compressive Strength, Modulus of Elasticity and Poisson's Ratio....40
3.5.2.2. 3 Point Bending Test with notched beams....41
3.5.2.3. Barcelona Test....43
4. RESULTS AND DISCUSSIONS....46
4.1. Fresh State Properties of Concrete....46
4.1.1. Unit Weight, Slump and Air Content....46

4.2. Hardened State Properties of Concrete 47
4.2.1. Compressive Strength 47
4.2.2. Elasticity Modulus and Poisson's Ratio 49
4.2.3. 3 Point Bending Test 51
4.2.4. Barcelona Test Results 56
5. CONCLUSIONS 62
REFERENCES 64
APPENDIX A: LOAD-CMOD CURVES FOR 3 POINT BENDING TEST 70

LIST OF FIGURES

Figure 2.1. History and predictions for future usage of composite materials [3] 3

Figure 2.2. Class of materials for composite production [3] 4

Figure 2.3. Young' Modulus, density values of some materials [4] 5

Figure 2.4. Characteristic curves for behavior analysis [3] 8

Figure 2.5. Interaction before and after loading and shear and tensile stresses [4] 11

Figure 2.6. Interfacial shear stress distribution after debonding [3] 12

Figure 2.7. Steel fiber types [7] 13

Figure 2.8. Effect of vibration on distribution of fibers [9] 14

Figure 2.9. Effect of fiber volume on workability [19] 17

Figure 2.10. Aggregates and concrete density [21] 21

Figure 3.1. Aggregate grading 34

Figure 3.2. Specimens in the curing pool 37

Figure 3.3. Test Setup for Compressive Strength, Modulus of Elasticity and Poisson's Ratio 41

Figure 3.4 3 point bending test setup 42

Figure 3.5. Attached metal apparatus and test setup 42

Figure 3.6. Test setup and a broken Barcelona test specimen 44

Figure 4.1. Average compressive strength values for each mixture 48

Figure 4.2. Average values of Modulus of elasticity 50

Figure 4.3 Average values for Poisson's ratio 51

Figure 4.4. Average values of f_{LOP} for each mixture (MPa) 52

Figure 4.5. Average values of flexural strength (MPa) 54

Figure 4.6. Average values of Toughness for each mixture 55

Figure 4.7. Average tensile strength of each mixture (MPa) 57

Figure 4.8. Average Toughness values (N*m) 59

Figure 4.9. Average G-BCN toughness values (N*m) 61

Figure A.1. Load-CMOD curves of LC specimens in 3 point bending test 70

Figure A.2. Load-CMOD curves of LCSF30-0.5 specimens in 3 point bending test 70

Figure A.3. Load-CMOD curves of LCSF30-1 specimens in 3 point bending test 71

Figure A.4. Load-CMOD curves of LCSF36-0.5 specimens in 3 point bending test 71

Figure A.5. Load-CMOD curves of LCSF36-1 specimens in 3 point bending test 72

Figure A.6. Load-CMOD curves of LCSF60-0.5 specimens in 3 point bending test 72

Figure A.7. Load-CMOD curves of LCSF60-1 specimens in 3 point bending test 73

Figure A.8. Load-CMOD curves of different volume fractions of fibers for LCSF30 series ..73

Figure A.9. Load-CMOD curves of different volume fractions of fibers for LCSF36 series ..74

Figure A.10. Load-CMOD curves of different volume fractions of fibers for LCSF60 series.74

Figure A.12. Load-CMOD curves of different fiber length for 1% fibers 75

Figure A.11. Load-CMOD curves of different fiber length for 0.5% fibers 75

LIST OF TABLES

Table 3.1. Chemical Composition of Silica fume (%) 30

Table 3.2. Physical Properties of Silica Fume 30

Table 3.3. Properties of Aggregates 31

Table 3.4. Properties of Steel Fibers 32

Table 3.5. Sieve Analysis of Aggregates 33

Table 3.6. Mix Proportions ($kg/m3$) – SP: Superplasticizer 36

Table 4.1. Unit weight and Slump Values 46

Table 4.2. Compressive Strength of Each specimen (MPa) 47

Table 4.3. Modulus of elasticity of each specimen (GPa) 49

Table 4.4. Poisson's Ratio Values 50

Table 4.5. f_{LOP} values for each specimen (MPa) 51

Table 4.6. Results of Flexural Strength for each specimen (MPa) 53

Table 4.7. Values of Toughness for each specimen (N*m) 55

Table 4.8. Fracture Energy Values (N/m).....56

Table 4.9. Tensile strength of each specimen (MPa).....56

Table 4.10. Toughness for different TCOD values (N*m).....58

Table 4.11. Average Toughness for different TCOD values (N*m) and coefficient of variations.....58

Table 4.12. G-BCN toughness for each specimen at different axial displacement (N*m).....60

Table 4.13. G-BCN average toughness values and coefficient of variations (N*m).....60

LIST OF SYMBOLS

A	air content by percentage in concrete
$A_{eff.}$	effective cross-section
D	measured concrete density
D	diameter of fibers
d_f	diameter of fibers
G_F	fracture energy
g	gravitational constant
L	length of fibers
l	length of fibers
l_c	critical transfer length
m	weight of the beam
P	load
S	span of the beam
T	calculated theoretical concrete density
U	length of the beam
V_f	fiber volume fraction
V_m	matrix volume fraction
W_0	toughness
δ_0	final deflection
η_l	coefficient of fiber length
η_θ	coefficient of fiber orientation
σ_{ct}	tensile strength of composite

σ_{mt}	tensile strength of matrix
σ_{fu}	tensile strength of the fiber
τ_{au}	adhesional shear bond strength
τ_{u}	maximum frictional shear stress
τ_{fu}	frictional shear bond strength

LIST OF ACRONYMS/ABBREVIATIONS

ASTM	American society for testing and materials
BC	Before Christ
C-S-H	Calcium silicate hydrate
CMOD	Crack mouth opening displacement
E(TCOD)	Energy absorption of concrete by total circumferential opening displacement
FRC	Fiber reinforced concrete
G-BCN	Generalized Barcelona test
HSLWAC	High strength lightweight aggregate concrete
LC	Plain concrete (without fibers)
LCSF30-0.5	Lightweight concrete reinforced with steel fiber of 30mm length with 0.5% volume fraction
LCSF30-1	Lightweight concrete reinforced with steel fiber of 30mm length with 1% volume fraction
LCF36-0.5	Lightweight concrete reinforced with steel fiber of 36mm length with 0.5% volume fraction
LCF36-1	Lightweight concrete reinforced with steel fiber of 36mm length with 1% volume fraction
LCF60-0.5	Lightweight concrete reinforced with steel fiber of 60mm length with 0.5% volume fraction
LCSF60-1	Lightweight concrete reinforced with steel fiber of 60mm length with 1% volume fraction
LCE	Extra plain concrete without capping
LECA	Lightweight expanded clay aggregate
LVDT	Linear variable differential transformer
LWA	Lightweight aggregate

LWAC	Lightweight aggregate concrete
LWASFRC	Lightweight aggregate steel fiber reinforced concrete
NWA	Normal weight aggregate
NWAC	Normal weight aggregate concrete
NWC	Normal weight concrete
OD	Oven dry
OPBC	Oil-palm-boiler-clicker
PVA	Pulverized fly ash
SCC	Self compacting concrete
SCLC	Self compacting lightweight concrete
SF	Steel Fiber
SP	Superplasticizer
TCOD	Total circumferential opening displacement
UNE	Asociación Española de Normalización
VMA	Viscosity modify agent

1. INTRODUCTION

Detailed understanding of mechanical properties and behavior of composites required for engineering applications of materials. The aim of this thesis is the investigation of the mechanical and fracture properties of pumice lightweight fiber reinforced concrete.

Throughout this work 7 different types of materials used; namely cement, silica fume, fine and coarse aggregates (sand, gravel and pumice), steel fibers, superplasticizer and also standard tap water were used for the production of steel fiber reinforced pumice lightweight aggregate concrete.

All specimens were made based on the same concrete mix proportions. Three different types of fiber were investigated, steel fibers (SF) of different length with hook-ends in two fiber contents of 0.5% and 1.0% by volume. As a control group, additional plain lightweight concrete batches were made.

Aggregate proportions were chosen to be 50% for sand, 15% for crushed gravel and 35% for pumice by total weight of aggregates. (35% for sand, 10% for crushed gravel and 55% for pumice by total aggregate volume). Natural sand, crushed gravel and pumice have been heated for 48 hours in a drying oven at 100-105 °C temperature before production to reach oven dry (OD) status.

Two different types of molds used throughout the research. For bending tests 100x100x500mm prisms and for compression tests, Poisson's ratio/modulus of elasticity and Barcelona tests Φ150x300mm cylinders were oiled and prepared for casting.

Modulus of Elasticity and Poisson's ratio were conducted with compression tests in accordance with related standards. The three-point bending test and Barcelona tests were used to determine the tensile strength and toughness of the specimens and to evaluate its behavior in post-cracking phase.

It is found that in order to obtain sufficient workability when adding fibers in the concrete, the addition of superplasticizers is needed. Capping affects the compressive strength results. It is observed that adding fibers have inconsistent effect on compressive strength. Similar results were also found in literature. On the other hand, adding fibers has no significant effect on the Modulus of Elasticity and Poisson's ratio.

After evaluating the results of the bending and double punch (Barcelona) tests, it is clear that all specimens developed significant ductile behavior during the post cracking phase. It is observed that steel fibers, with high enough aspect ratio, significantly contribute to tensile properties and toughness of the specimens.

In conclusion, it is determined that the increase of fiber content and aspect ratio, greatly enhances the mechanical and fracture properties of the pumice lightweight steel fiber reinforced concrete.

2. LITERATURE REVIEW

2.1. Composite Materials

Introduction of 2 or more materials in a body, to achieve improved properties of an outcome material has a long history starting around 1500 B.C to today (Fig 2.1). One of the first examples given as composite materials are addition of sweat to mud bricks by Mesopotamian people, invention of composite bows used by the archers of Cengiz Han and so on and so forth. A milestone for modern composites was the discovery of glass fibers in 1930's by a glass company based in U.S.A. Although composite materials were already considered as one of the most prominent construction materials such as wood, reinforced concrete and so on, the ongoing trend of using metals and alloys in construction business especially after introduction of steel in 19th century kept increased until after 2 decades of invention of glass fibers, in post-world war II era in 1950's, when applications of military and aerospace engineering fields created the demand of high-strength, light-weight but also ductile materials resistant to high temperatures for the production of aircrafts, rockets and etc., which was responded by the inclining polymer industries with their improved understanding of plastics and ceramics. [1][2][3]

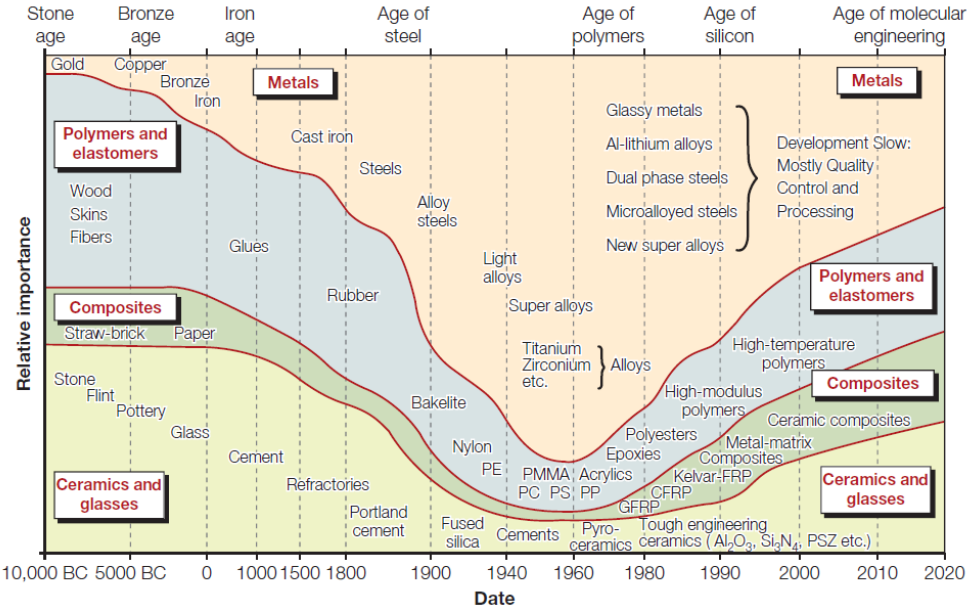

Figure 2.1. History and predictions for future usage of composite materials [3]

In a straightforward manner, the word *composite* suggests the existence of a high strength, fibrous, laminated or particulate form of, arbitrary or predesigned distribution of material(s), in a relatively less stiff medium which is called *matrix* [2,4]. The resultant composite material carries the properties of its constituent materials. Hence the selection of the constituent materials is highly dependent on the engineering application. There are different types of materials (Figure 2.2) available for the engineers to design and respond to a specific engineering problem. One of the most important mechanical properties of composite materials is the high stiffness to weight ratio. We can see elasticity modulus to density chart of some of the most prominent materials that are either used as matrix or reinforcement in Figure 2.3. [4].

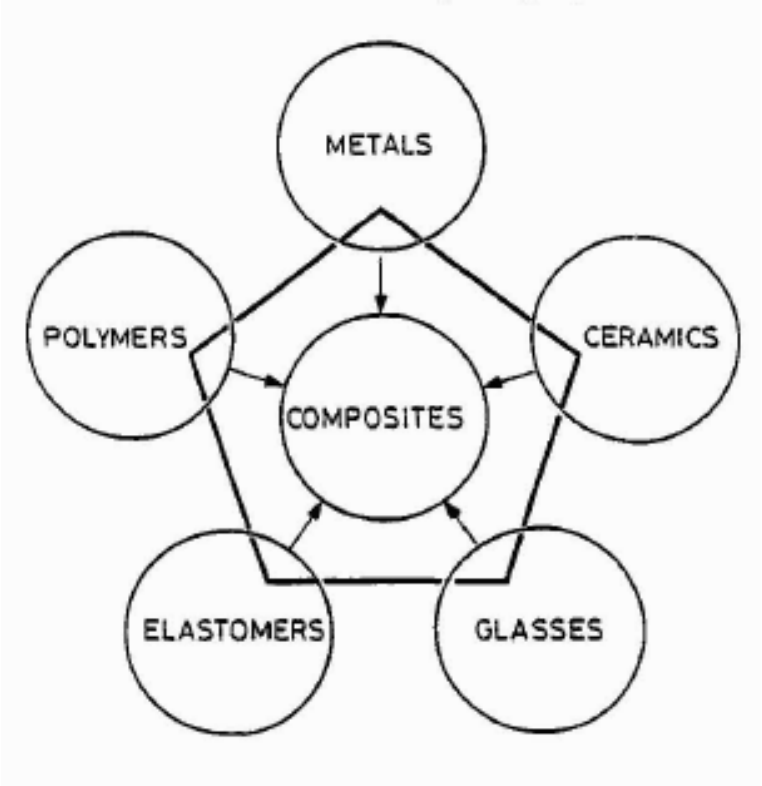

Figure 2.2. Class of materials for composite production [3]

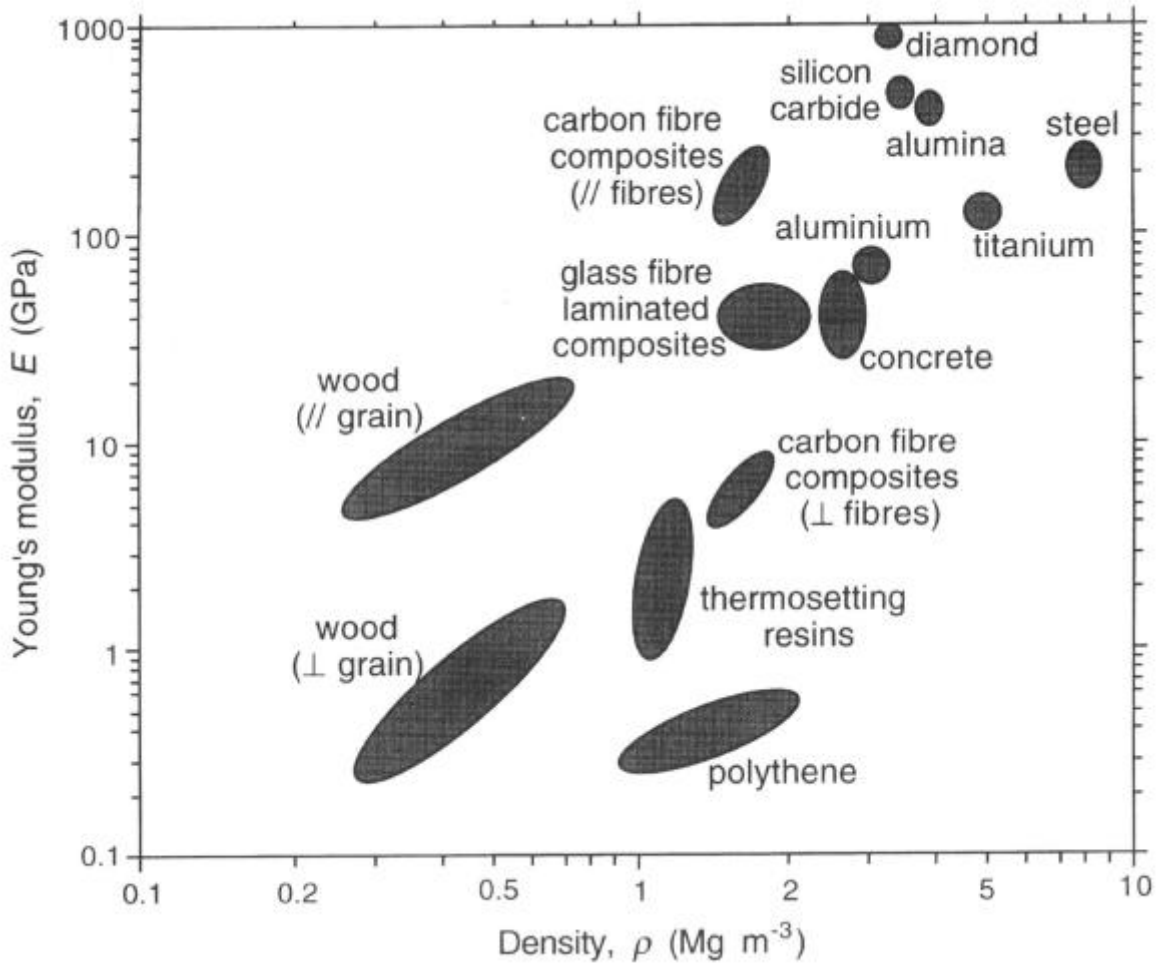

Figure 2.3. Young' Modulus, density values of some materials [4]

2.1.1. Fiber Reinforcement

One of the most preferred forms of using reinforcement in composite materials is fibrous form. It is well known that most of the materials have better mechanical properties in fibrous forms compared to bulk forms including stiffness, strength and last but not least density. This phenomenon can be easily understood considering size effect phenomenon which results lesser flaws in material due to smaller size or by the inhibited orientation of the molecules of such materials onwards fiber direction. [5]

Fiber reinforcements, as well as other types of reinforcements, have usually superior thermal and electrical conductivity. Besides this, most of the fiber reinforcements are creep resistant. Fiber reinforcement brings forth the design flexibility to the engineer to respond according to directionality of the loading [6]

It is possible to categorize fibers according to their chemical components, dimension and strength/stiffness properties. Most common fiber types are Metal, Polymeric, Ceramic, Graphite, Natural etc. [5][6][7].

2.1.2. Matrix

A binding type of material is required for fibers to be held together but not disperse. Such binding materials, i.e., matrices, are constituent materials for composites, since fibers themselves are not sufficient enough to carry transverse or compressive loadings. Fibers are also vulnerable to external attacks such as wear/corrosion. Hence matrix materials surround the fibers in order to maintain a structural element that can be used in different engineering applications [2][5].

As it is for concrete to reinforcement bars, matrix materials partake in defending fibers against external attacks, transferring external loads to the fibers along fiber - matrix interfaces, or simply -but of utmost importance- in carrying transverse loads [5].

There are different types of materials available such as *Metallic, Ceramic or Polymer* based materials [5].

It is not the only design approach to choose proper mechanical properties of constituent materials independent of each other for a given engineering problem but also the interaction between fibers and matrix shall be considered. Matrix – Fiber compatibility is an important matter for engineers since most of the polymeric composite materials are being subjected to high temperatures during manufacturing or through their service life. Hence choosing two or more materials with different thermal conductivities may create

residual stresses that will eventually have a significant effect on mechanical behavior of the composites. [2][4][7].

2.1.3. Matrix – Fiber Interface

Matrix – Fiber interface plays a great role for composite materials, since they are the medium of interaction between these two constituent materials. Several chemical or physical bonding processes occur at the interfaces depending on the selection of constituent materials. Especially for polymer based composites time dependent chemical reactions and wetting phenomenon between liquid/solid interfaces are such bonding mechanisms to be observed [4].

There are mainly three types of interaction between the fibers and the matrix [8]:

(i) Physical and chemical adhesion
(ii) Friction
(iii) Mechanical anchorage

For fiber reinforced cementitious composites, the frictional and adhesional bondings are generally weak. They play an important role, however, especially for advanced cementitious matrices where water/cement ratio is very low and for composites with high surface area fibers. For conventional fiber reinforced composites with high water/cement ratio and fibers having the diameter of 0.1 mm and above, adhesional and frictional bonding is not sufficient to have an effectively working composite. Hence additional interaction is supplied by mechanical anchoring. There are several fiber types available for this purpose (see chapter 2.2) [8].

A common procedure of analysis for predicting the bonding mechanisms is single fiber pull-out test. The purpose of the test is to obtain pull-out vs. slip relation. The characteristic curves between interfacial shear stress vs. pull-out displacement demonstrate

the failure mode of the composite. Most of the models assume a constant frictional shear behavior Fig 2.4 [8].

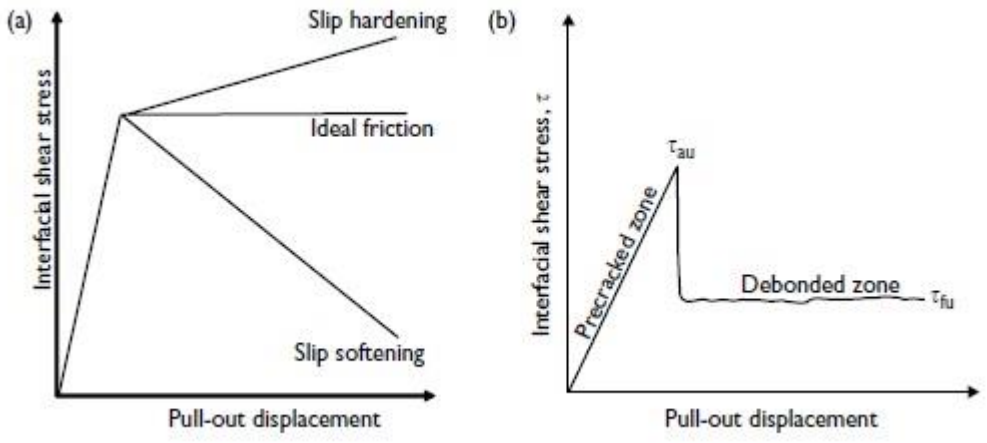

Figure 2.4. Characteristic curves for behavior analysis [3]

Fiber-matrix interaction occurs in a small volume of the matrix that covers the fiber. Bulk matrix structure differentiates from the structure of this small volume, hence particular effects cannot be predicted using such analytic models since these models assume a uniform matrix down to fiber surface. Interaction mechanisms that cause stress transfer allow for prediction of stress-strain curve of the composite and hence it's ductile or brittle failure behavior. Understanding these mechanisms serves the basis for designing high performance composites mostly through changing fiber geometry for improved fiber-matrix interaction [8].

Stress-transfer mechanisms should be investigated for both pre-cracking stage and the post-cracking stage for brittle matrix composites where the processes significantly differ for two cases. For pre-cracking stage, the longitudinal displacements of constitutive materials assumed to be geometrically compatible. In this stage, the dominant mechanism is elastic stress transfer. Elastic moduli of the constitutive materials differ, hence shear stresses that developed at the interface are responsible for dispense of external loads between the fibers and the matrix for the sake of keeping the strains of these materials same at the interface. The first crack stress of the composite and the limit of proportionality

can be predicted through this elastic shear transfer since it is the most dominant mechanism that takes place. Along the fiber-matrix interface, the distribution of elastic shear stresses is non-uniform [8].

The dominant stress transfer mechanism changes into frictional slip due to debonding that occurs at the interface as loading increase. At this stage relative displacements take place between the fiber and the matrix. At the fiber-matrix interface, it is assumed that uniformly distributed frictional shear stresses occur. In later stages of loading where fiber bridging begins to develop after cracking, this process is the dominant mechanism. Frictional shear transfer mechanisms are considered to predict such mechanical properties as the ultimate strength and strain of the composite [8].

As the loading continues, the interfacial shear stresses exceed fiber-matrix shear strength and transition of stress transfer mechanism from elastic stress transfer to frictional stress transfer occurs. Exceeded fiber-matrix shear strength is called adhesional shear bond strength, τ_{au}. After fiber-matrix debonding occurs, frictional shear stresses act through the fiber-matrix interface in the debonded zone. τ_u is the maximum frictional stress, so-called frictional shear strength. The values of τ_{au} and τ_u may differ according to failure mechanism of the composite. τ_u takes a higher value for slip hardening cases whereas for slip softening cases, it takes a lower value then τ_{au} [8].

In the case that the tensile strength of the matrix is higher than fiber-matrix adhesional shear strength, debonding may occur before cracking begins. In such case, elastic stress transfer and frictional stress transfer mechanisms affects the process together. The shape of stress-strain curve before cracking of the matrix is also influenced by this combined effect. Cracking of the matrix occurs prior to fiber debonding in case that the matrix has a low tensile strength value. For such case, an analytical method based on fracture mechanics shall be assumed [8].

2.1.3.1. Pre-cracked stress transfer. Elastic stress transfer models are referred as *shear lag theories.* The stress field in the vicinity of a discontinuous fiber analyzed in these models. There are several assumptions made in order to calculate this stress field:

(i) Both the fiber and the matrix are elastic.
(ii) The interface is infinitesimally thin.
(iii) Perfect bond exists at the interface of the fiber and the matrix.
(iv) The properties of the matrix are uniform.
(v) The fibers are arranged in a regular, repeating array.
(vi) Tensile strain of the composite is equal to tensile strain in the matrix at a distance *R* from the fiber.
(vii) There is no stress transfer at the fiber ends.
(viii) Neighboring fibers stress fields do not influence one another.

The value of shear stress decreases from the ends of the fiber towards the center where it drops to zero at interface as it is presented in Figure 2.5. The stress transfer from the matrix to fiber takes place at the ends of the fiber and tensile stress gradually increases towards the middle where it takes its maximum value. The maximum value of tensile stress that can be transferred to fiber is the yield or tensile strength of the fiber. *Shear lag theories* are used to calculate shear stresses distributed at the interface for the sake of achieving this maximum tensile strength of the fiber [8].

For pre-cracking stage, the longitudinal displacements of constitutive materials assumed to be geometrically compatible. In this stage, the dominant mechanism is elastic stress transfer. Elastic moduli of the constitutive materials differ, hence shear stresses that developed at the interface are responsible for dispense of external loads between the fibers and the matrix for the sake of keeping the strains of these materials same at the interface

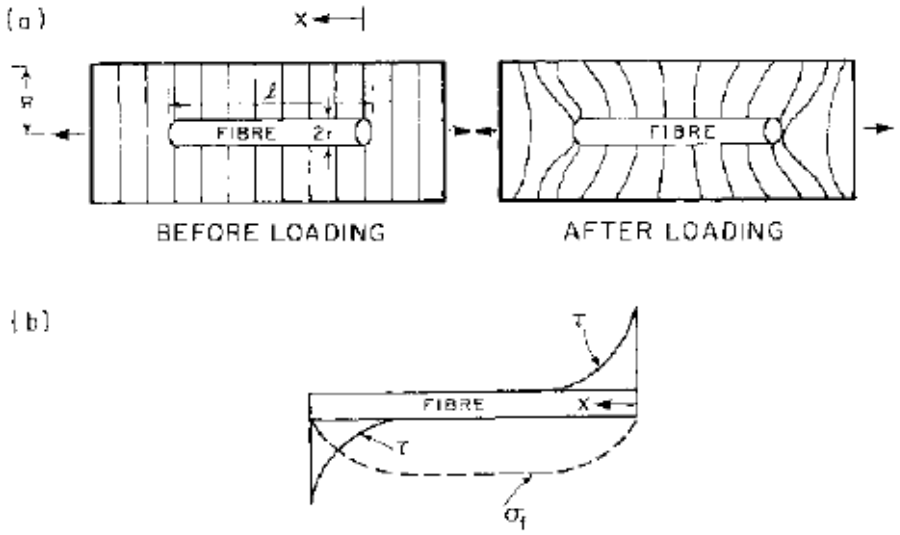

Figure 2.5. Interaction before and after loading and shear and tensile stresses [4]

2.1.3.2. Post-crack stress transfer. In the post-crack zone, fibers cause a bridging effect across the propagating crack mouths in the brittle matrix. The mechanism that occurs through this bridging effects controls stress-strain curve hence determines the ultimate strength and mode of failure of the composite. Pull-out tests are simulations for such bridging effects that are applied both analytically and experimentally [8].

The stress transfer mechanisms for cracked composites are, again, elastic bonding and frictional slip as for the uncracked composites. However in the cracked composites, the maximum interfacial shear stress values occur at the point where the fiber enters the matrix. In case that debonding already occurred at the point where fiber enters the matrix, a combined mode of shear stress distribution will occur. At the debonded zone, frictional shear stresses will act whereas towards the fiber ends, a decreasing elastic shear stress would be observed (Figure. 2.6). If cracking occurs prior to debonding, dominant stress transfer mechanism will be elastic shear stress transfer [8].

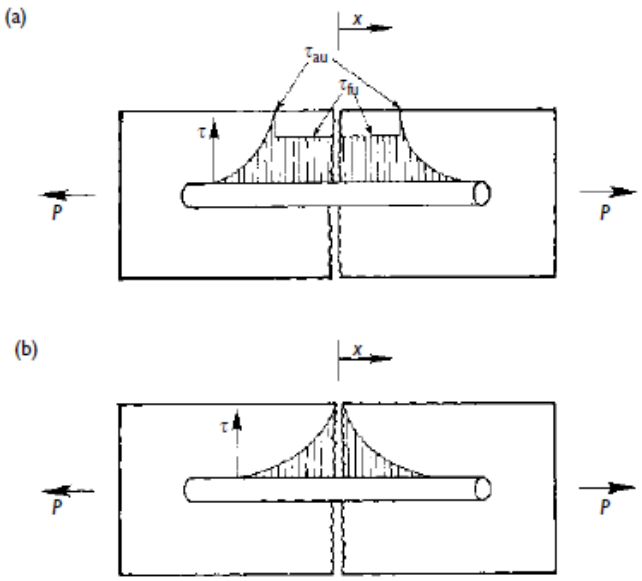

Figure 2.6. Interfacial shear stress distribution after debonding [3]

Debonding will occur once the elastic shear strength is exceeded at the intersection point where fiber enters the matrix. If the debonding occurs only in some part of the fiber where elastic shear stress exceeds the adhesional shear bond strength, stress transfer mechanism in debonded zone will be that of frictional slip where at the rest of the fiber it will be elastic shear transfer. This suggests that total failure of the composite will not necessarily occur once the shear bond strength exceeded [8].

2.2. Steel fiber usage in composite materials

Even though fiber reinforced composites have a long history, introduction of fibers into cement paste happened only in 1874 [9]. Usage of discontinues steel fibers such as nails, wire segments and metal chips to improve the mechanical properties of the concrete dates back to 1910. In early 1960's the potential of steel fibers as a reinforcement for concrete realized in United states which resulted dozens of research and investigation until this day [10].

In general, there are 5 types of steel fibers according to their production methods [11]:

(i) Cold-drawn wire
(ii) Cut sheet
(iii) Melt-extracted
(iv) Mill cut
(v) Modified cold-drawn wire

There are several different types of steel fibers available according their geometrical properties such as length, diameter, cross sectional shape and surface damage. Circular, elliptical, rectangular cross sections are some available shapes, yet dominant cross section that is used is the circular. In order to have mechanical anchorage, fiber surface can be treated or deformed. Ring or clip types of fibers are also available for engineering design (Fig 1.7) [11].

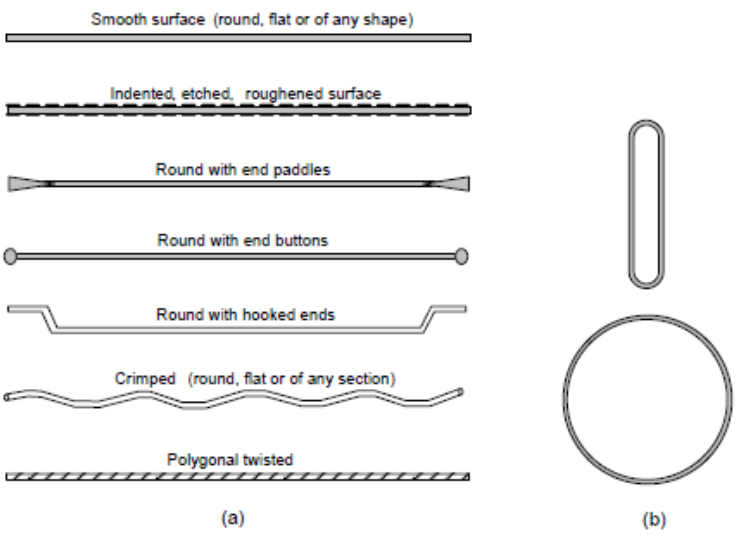

Figure 2.7. Steel fiber types [7]

2.2.1. Fiber orientation and distribution

It is expected that the fibers are randomly orientated and uniformly distributed through the composite material. However, after mixing, placing and vibration processes, this assumption does not represent the real cases. One of the most common methods for placing the mix in the moulds is using table vibrator. When table vibrators are used, fibers mostly become aligned in horizontal planes (Fig 1.8). Besides, fibers tend to move down in the specimen or move close to the sides of the moulds. This phenomenon is called “wall effect” [8].

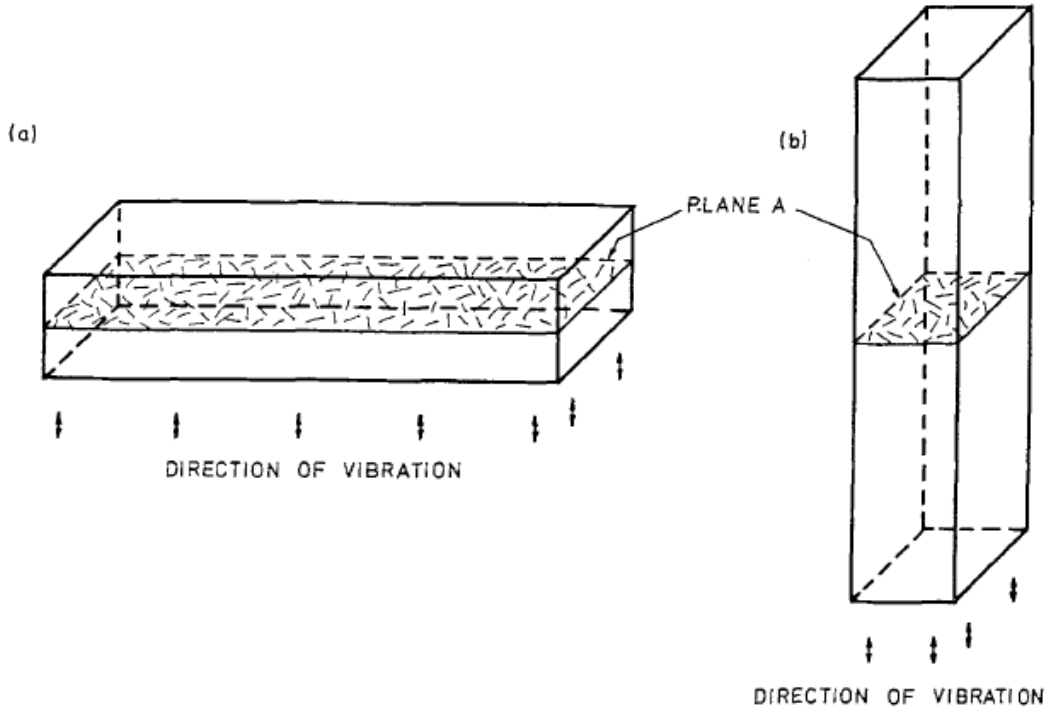

Figure 2.8. Effect of vibration on distribution of fibers [9]

Fiber orientation becomes more prominent when the direction of loading considered. If fibers are perpendicularly oriented considering the direction of loading, they will have no contribution to carrying the load.

The effect of fiber orientation can be shown on the grounds of "Rule of Mixture". Assuming perfect bond between fibers and matrix, tensile strength of the composite can be calculated as follows [13]:

$$\sigma_{ct} = \eta_l \eta_\theta V_f \sigma_{fu} + V_m \sigma_{mt}$$

Where,

η_l : Coefficient of fiber length

η_θ : Coefficient of fiber orientation

σ_{ct} : Tensile strength of the composite

σ_{mt}: Tensile strength of the matrix

σ_{fu} : Tensile strength of the fiber

V_f : Fiber volume fraction

V_m : Matrix volume fraction

Fiber length coefficient η_l is given by:

For $l < l_c \quad \eta_l = \frac{1}{2l_c}$

For $l \geq l_c \quad \eta_l = 1 - \frac{l_c}{2l}$

Where l is the fiber length and l_c is the critical transfer length. Assuming constant interfacial shear stress transfer for frictional stress transfer, l_c given as:

$$l_c = \frac{\sigma_{fu} d_f}{2\tau_{fu}}$$

Where d_f is fiber diameter and τ_{fu} is frictional shear bond strength between fiber and matrix.

There are several models proposed for calculating, η_θ, fiber orientation coefficient and its effect on tensile strength of the composite in the literature [14, 15, 16, 17].

Abrishambaf *et al*. [18] investigated the influence of fiber orientation on tensile behavior of ultra-high performance fiber reinforced cementitious composites. They employed a magnetic field during casting to have fibers parallel (0*), perpendicular (90*) and randomly oriented to the direction of loading in uniaxial tensile stress test. They used two different volume fractions of steel fibers: 1.5% and 3%. They reported that fiber orientation has a significant influence on the tensile behavior of the material. They observed that influence of fiber orientation had greater impact on tensile strength than increasing fiber content from 1.5% to 3%.

2.2.2. Workability

Addition of fibers into mixture decreases the workability (Figure 2.9). With water-absorbent fibers the effect may even increase compared to addition of non-water-absorbent fibers. Workability is a critical issue for fiber-reinforced concretes since it imposes limitations on fiber content and final (after mixing) fiber aspect ratio. Factors associated with maximum fiber content and acceptable workability of the mixture are fluidity and volume fraction of the cement paste, the maximum size of the coarse aggregate and fiber aspect ratio [19].

In order to achieve maximum benefit of addition of fibers, good fiber distribution and orientation is necessary. Fiber balling or fiber clumping is a phenomenon that occurs when the fibers are not sufficiently distributed in the matrix. Fiber balling may block fibers and can impose limitation of movement on them. Workability is at most importance in order to achieve uniform distribution of fibers. Reduced workability may influence mechanical properties of composites and efficiency of fibers negatively due to non-

uniform distribution of the fibers. Workability also controls the casting of the mixture without segregation of aggregates. Water/cement ratio and content of superplasticizers are the most prominent parameters that control workability [20].

The negative effect of addition of fibers mostly evaluated with two important parameters: Volume fraction,V_f, and aspect ratio, L/D, of fibers. Since increase in both volume fraction and aspect ratio causes further reduction in fresh mix properties of concrete, a proposed parameter so-called fiber factor which is the multiplication of volume fraction and aspect ratio is proposed [26].

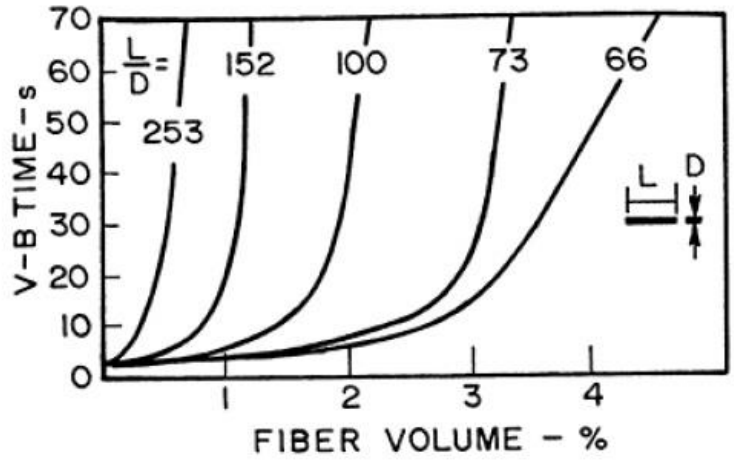

Figure 2.9. Effect of fiber volume on workability [19]

Bayasi and Soroushian [26] investigated the effect of fiber factor of different type of steel fibers on workability. They used straight-round, crimped-round, crimped-rectangular, hooked and hooked-collated steel fibers with different volume fraction and aspect ratio in order to characterize the workability of the mixtures. They reported that increase in fiber factor has a negative effect on workability in general. For the same fiber factor, crimped fibers have slightly higher slump values, where for the straight fibers the inverted slump time is slightly lower. On the other hand hooked fibers generate inverted slump cone times that are slightly higher than straight and crimped fibers. When Vebe times are considered, crimped fibers give slightly lesser rate compared to straight fibers for the same fiber factor.

Last but not least, hooked and crimped fibers increase the air content of the mix more than straight fibers.

Chu *et al.* [27] investigated the effect of fiber factor on fresh and hardened states of steel fiber, fiber reinforced concrete (FRC). They used four different types of hooked steel fibers with different geometries. They suggested several alternative fiber factors besides $V_f\,{}^{L}/_{D}$ that are $V_f({}^{L}/_{D})^2$, $V_f({}^{L_d}/_{D})^2$, nL^3, ${nL_d}^3$ where n is the number of fibers in the mixture and L_d is developed length of hooked fibers. They reported that increase in fiber volume decreased workability in general. They also reported that considering a fiber factor function of volume fraction $V_f({}^{L}/_{D})^2$gives better correlation for slump values and for a fiber factor function of number of fibers nL^3 corresponds to best fit compared to classic fiber factor $V_f\,{}^{L}/_{D}$. They observed that cylinder strength and young modulus increased while Poisson's ratio decreased with increasing volume fraction. Finally they reported that $V_f({}^{L}/_{D})^2$gives the best fit as a fiber factor function of volume fraction and $nL^3D^{0.5}$ gives even better correlation for hardened concrete properties.

2.2.3. Effect on Mechanical Properties

Addition of steel fibers has great influence on mechanical properties of composites depending on the type and volume fraction of the fibers used. In general, depending on the volume fraction of the fibers, there are three classes of fiber-reinforced composites. Composites may have low volume fraction of fibers (< 1%), moderate volume fraction of fibers (1% to 2%) and high volume fraction of fibers (>2%). It has been noted that with addition of steel fibers up to 1 - 1,5% of volume, increases the tensile strength, flexural strength and compressive strength of the composite up to 100%, 150-200%, 10-25% respectively. Besides addition of fibers increases impact strength and toughness hence increases the ductility of the composite [21]

Abbass *et al.* [28] investigated the effect of steel fibers with different geometries and volume fraction on the mechanical properties of steel fiber reinforced concrete with

different water/cement ratios. They utilized hooked steel fibers with 40, 50 and 60 mm length and 65, 80 and 80 aspect ratios respectively. They successfully produced specimens with compressive strength up to 93 MPa, 75 MPa, and 66 Mpa for water/cement ratios of 0.25, 0.35 and 0.45 respectively. They reported that with the increase of fiber volume fraction from 0.5% to 1.5%, compressive strength of the specimens with moderate strength increased from 10% to 25% and direct tensile strength increased from 11% to 47% respectively. For specimens with fiber aspect ratio of 65, flexural strength increased from 3% to 124% for 0.5% and 1.5% volume fractions whereas for the higher aspect ratio of 80, flexural strength increased up 140%.

Song *et al.* [29] investigated the effect of steel fiber volume fraction on high-strength fiber reinforced concrete. They produced specimens with four different volume fractions of 0.5%, 1.0%, 1.5% and 2.0%. They reported compressive strength values of 85, 91, 95, 98 and 96 MPa, splitting strength values of 5.8, 6.9, 8.7, 10.8 and 11.5 MPa and modulus of rupture 6.4, 8.2, 10.1, 12.3 and 14.5 MPa for plain concrete, 0.5%, 1%, 1.5% and 2.0% volume fractions respectively. They observed a steady increase in toughness indexes with increasing volume fractions.

Iqbal *et al.*[30] investigated the effect of micro steel fiber content on the properties of high strength lightweight self-compacting concrete. They reported that plain concrete strength was up to 67.8 Mpa whereas with 1.25% fiber content it decreased to 59.74 MPa. The reduction in compressive strength is a common phenomenon that occurs due to increased air content in the mixture due to addition of fibers. They observed that the increase in splitting tensile strength was around 37% with increase of fiber content from plain concrete to 1.25% volume fraction. Furthermore they reported that there was no significant change in modulus of elasticity of the specimens due to increase in fiber content. Finally the flexural strength of the concrete increased up to 110% with the increase in fiber content from plain concrete to 1.25% volume fraction.

2.3. Lightweight Aggregates in Composite Materials

Utilization of lightweight aggregates for structural purposes dates back in history. Pumice is one of the oldest types of lightweight aggregate that is being used still today. In short we can separate two groups of lightweight aggregates being; natural aggregates and man-made aggregates [22]. Earlier natural lightweight aggregates were mostly volcanic such as pumice, tuff, scoria etc. These types of aggregates were used as both fine and coarse aggregates. When they are used as fine aggregates, they do behave as pozzolanic materials. They have the capacity to interact with lime during hydration processes which results the production of calcium silicate hydrate (C-S-H). As it is well known, C-S-H strengthens the material, modifies porous structure and boosts the durability properties [22].

Several techniques were established due to increasing demand and non-availability of lightweight aggregates in different geographies. One way is to use natural raw materials such as clay, slate, shale, etc. Another method is to use industrial by-products such as fly ash, bed ash and blast furnace slag etc. The properties of aggregates depend on the raw material or the process applied for the production of them [22].

2.3.1. Lightweight Aggregate Concrete (LWAC)

There are several advantages of using lightweight aggregate concrete (LWAC) for structural purposes. LWAC has high strength/weight ratio. Reducing the dead weight of the structure causes decrease in earthquake forces that may act on the structure. Furthermore LWAC's have good tensile strain capacity, high durability and low coefficient of thermal expansion [21]. Other advantages of LWACs can be counted as: reduction at the dimension of the structure and foundation, design flexibility for tall buildings and long spans, ease of handling of components, reduction in construction costs [21][22][23][24].

There is a wide range of different densities for lightweight aggregates (LWA) from 50 kg/m^3 for expanded perlite to 1000 kg/m^3 clinkers (Figure 2.10) [22]. Although low density LWA's are not preferred for structural members since they have low strength, they have superior heat and sound insulation characteristics [21].

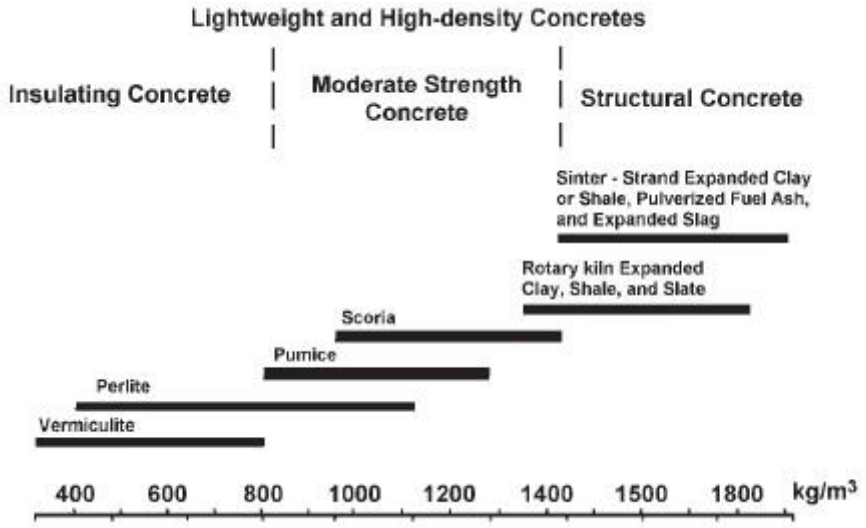

Figure 2.10. Aggregates and concrete density [21]

However, several disadvantages of LWAC's restricted their usage as load carrying structural members in the construction industry. For the same mix proportion and compressive strength, normal weight concrete (NWC) has higher ductility than LWAC. Besides this, in general, the mechanical properties of LWAC are lower than NWC. In recent studies, high strength lightweight aggregate concrete (HSLWAC) with high compressive strength (up to 50 – 100 MPa) has been produced using several different types of LWAs. Nonetheless brittleness of LWAC in compression and tension increases with higher concrete strength. One way to improve the mechanical properties and ductility of LWAC is to introduce fibers in the mixture [21].

2.3.2. Fresh State Properties of LWAC

Kim *et al.* [31] investigated the effect of two types of lightweight aggregates on self-consolidating concrete. They used normal density crushed limestone for control mix and two LWAs produced from different raw materials: one of them being rhyolite fine powder (density of 1.58 g/cm^3) and the other type was produced from wastes of screening sludge (density of 2.07 g/cm^3). They conducted several experiments to evaluate fresh state properties of mixtures such as slump-flow, V-funnel and U-box tests. They reported that flowability of self-consolidating concrete increase as the density of LWA decreases. For the mixture produced with rhyolite fine powder, flow through the V-funnel time increased as the ratio of LWA replaced with normal weight aggregate (NWA) increased. They observed that segregation resistance of self-consolidating concrete decreases as the density of LWA gets a smaller value. Finally they reported that filling ability of self-consolidating concrete was not influenced by different densities of LWA.

Lo *et al.* [32] investigated fresh and hardened properties of self-compacting lightweight concrete (SCLC) compared to self-compacting concrete (SCC) with normal weight aggregates. They used different proportions of binder, fine and coarse expanded shale aggregates as LWA, pulverized fuel ash (PVA) as an additional binder to increase the viscosity. They also utilized superplastizer (SP) and viscosity modify agent (VMA) to improve the workability of the concrete. They reported that slump-flow of SCLC increased with the increase in binder content due to the positive effect of PVA on workability. They observed that lesser SP and VMA content are needed for SCLC to have the same slump-flow with SCC. They conducted L-box test to evaluate passing abilities of both SCLC and SCC. They reported that that T_{40} values decreased with increasing binder content however there is a limit value for binder content of which even though the flowability of the paste increases, there is no further improvement on passing abilities.

Shafigh *et al.* [33] run a comparative work for investigating fresh and hardened properties of normal weight and lightweight aggregate concrete. They utilized two types of LWAs: oil-palm-boiler-clinker (OPBC) and lightweight expanded clay aggregate (LECA). Normal weight granite aggregates were used for NWAC. Slump values of mixtures with

NWA, OPBC and LECA found 105, 55 and 50 mm respectively. They reported that significant reduction with OPBC may be due to irregular shape and high porous surface texture compared to granite aggregates. Such porous structure results absorption of water and cement paste which in turn reduces slump values. Kockal and Ozturan [34] reported that such reduction in slump values for LWAC compared to NWAC occurs also due to lesser gravitational work done since the mixture of LWAC is relatively lighter. Hence LWAC may have accepted workability even though low slump values.

2.3.3. Mechanical Properties of LWAC

Zhang and Gjørv [25] produced high-strength lightweight concrete with five different types of LWA, four types of being expanded clay and one type of sintered fly ash. They successfully produced LWAC with fresh concrete density and 28-day compressive strength varied from 1595 to 1880 kg/m^3 and from 57.3 to 102.4 MPa, respectively. They reported that different types of lightweight aggregates with different particle density and water absorption characteristics are the primary factor regulating the compressive strength. Furthermore, they observed that compressive strength increases with increasing concrete density. Consistently with the increase of compressive strength, they also reported that flexural and splitting tensile strength increased from 5.4 to 7.3 MPa and from 3.5 to 5.6 MPa, respectively. For the same compressive strength, it is noted that LWAC has lesser flexural and splitting tensile strength and also modulus of elasticity than that of NWAC.

Balaguru and Foden [26] produced steel fiber reinforced structural lightweight concrete with two different fiber lengths, having three different volume fractions and varied fine aggregate composition from all LWA to different percentages of LWA with sand. They observed that equilibrium density of the specimens are varied from 1537 to 1758 kg/m^3. Furthermore they observed that fiber addition increased density about 100 kg/m^3. They reported that all LWA mixes have the lowest compressive strength values whereas with the addition of fibers compressive strength increased. They successfully produced specimens with compressive strength up to 42 Mpa. Addition of fibers increased the modulus of elasticity up to 21.2 GPa whereas higher LWA proportions decreased the modulus. Furthermore they reported that increase in fiber content resulted increase in both

splitting tensile strength and flexural strength. Last but not least, increase in fiber content significantly improved the toughness of the specimens and resulted strain-hardening behavior.

Balendran *et al.* [23] investigated influence of steel fibers on mechanical properties of high-strength LWAC and normal weight aggregate concrete (NWAC) with different specimen sizes. They kept fiber volume fraction constant 1% for all the mixtures. Due to low volume fraction of the fibers, they observed no effect on density and compressive strength of the specimens. They reported that cylinder splitting tensile strength of FRC increased 100% for both LWAC and NWAC. Whereas flexural strength is increased 2.5 times for LWAC, there was no significant improvement for NWAC. They also observed a similar result for prism splitting tensile strength where the improvement for LWAC exceeded that of NWAC. They also reported that toughness indexes of LWAC are higher than that of NWAC.

Choi *et al.* [24] investigated the influence of different fibers on all-LWAC using both fine and coarse artificial LWAs on the mechanical properties. They used three different types of fibers: steel, vinyl and polyethylene. Furthermore they produced NWAC with same compressive strength values that of LWAC. They reported that addition of fibers had a positive effect on compressive strength besides the specimens with polyethylene fibers. They also reported that splitting tensile strength of LWAC increased by 31-98% whereas the increase for NWAC was only 18-46% and the effect of steel fibers exceeded other type of fibers. Positive effect of fibers was also higher in LWAC than NWAC for flexural strength. They observed that toughness of LWAC became comparable to that of NWAC with the addition of 1% fibers. They also reported that improvement on toughness due to addition of fibers in LWAC exceeded that of NWAC and the effect of steel fibers also was higher than other types of fiber.

2.4. Pumice Lightweight Aggregate Steel Fiber-Reinforced Concrete

In this current study, different volume fractions of pumice lightweight aggregates and steel fibers utilized to produce pumice lightweight aggregate steel fiber-reinforced concrete. There are several works in the literature with the same aim. I will first introduce the scope of these works and then report the results of hardened state properties.

Campione *et al.* [35] prepared three different mixtures with pumice stone, expanded clay and normal weight aggregate with different volume fractions of hook-end steel fibers namely 0.5%, 1.0% and 2.0%. Length, Diameter and aspect ratio of hook-end fibers are 30, 0.5 mm and 60 respectively. They used moderate size (3 to 7 mm) and great size (7 to 10 mm) pumice stone as coarse aggregate and kept sand as fine aggregate to improve the mechanical properties of the material. They prepared cylinder specimens and prism specimens with the dimension of 100 × 200 mm and 100 × 100 × 350 mm respectively.

Duzgun *et al.* [36] replaced four volume fractions of pumice aggregate that of 25%, 50%, 75% and 100% with normal weight aggregates and utilized three different volume fractions of hook-end steel fibers namely 0.5%, 1% and 1.5%. Length, diameter and aspect ratio of steel fibers are 60mm, 0.8mm and 75 respectively. They cast 16 different mixtures and for every mixture six cylinder specimens (150 × 300 mm) and three prism specimens (150 × 150 × 500 mm) were prepared.

Libre *et al.* [37] investigated the effect of hybrid steel and polypropylene fibers on the properties of pumice lightweight aggregate concrete. They utilized hybrid fibers as well as mixtures with steel fibers only. Due to relevance of the current study, only steel fiber results will be investigated. The weight ratio of pumice lightweight aggregate to natural sand kept constant (LWA/S = 0.56). They prepared six 150 mm cubes, four cylinders with 150 × 300 mm and three prisms with 150 × 150 × 500 mm dimensions for each mixture.

2.4.1. Compressive Strength and Elastic Modulus of Pumice LWASFRC

In the first study [35], it was reported that increase in fiber volume fraction did not have significant effect on compressive strength of concrete. They successfully produced specimens with compressive strength around 20 MPa. On the other hand from 0% volume fraction of fibers to 2%, elastic modulus decreased from 15.2 GPa to 13.4 GPa. They reported that this may be due to incompatibility of fiber and aggregate sizes which resulted lesser compaction of the concrete.

In the second study [36], they observed a decrease in compressive strength with the increase of pumice aggregate ratio. For 0% fiber volume fraction specimens, with the increase of pumice ratio of 50%, 75% and 100%, compressive strength decreased 21.7%, 43.1% and 79.2% respectively compared to normal strength concrete. However for 1.5% fiber volume fraction specimens, the reduction was 19.1%, 39.3% and 63.3% with the increase of pumice ratio from 50% to 75% and 100%. They reported a slight increasing trend in compressive strength with the increase of volume fraction of fibers. With 25% pumice ratio and increase in steel fiber content from 0% to 0.5%, 1.0% and 1.5%, compressive strength increased 2.9%, 7.1% and 10.4% respectively. With 100% pumice ratio with same trend of fiber content increase, compressive strength increased 9.3%, 15.8% and 21.1% respectively. They reported similar trends for elasticity modulus. Increase in pumice content decreases the elastic modulus whereas increase in steel fiber content increased the elastic modulus. They observed varying elastic modulus between 6.71 GPa to 11.38 GPa for different volume fractions of fibers and pumice respectively.

In the third study [37], they reported for fiber volume fractions of 0%, 0.5% and 1.0%, compressive strengths values were 18.7 MPa, 30.2 MPa and 28.9 MPa respectively. They observed inconsistent effect of fiber volume fraction on compressive strength.

2.4.2. Tensile Strength of Pumice LWASFRC

In the first study [35], they reported that with the increase in fiber content from 0% to 2%, splitting tensile strength increased from 1.93 MPa to 2.27 MPa with an increase of 3% and 18% respectively compared to normal weight concrete. They observed that increase in fiber content was not effective on tensile strength however post-peak strength increased significantly and very ductile behavior was also observed.

In the second study [36], they observed a significant increase in tensile strength with the increase of fiber content. With the increase of fiber volume fraction by 0.5%, 1.0% and 1.5%, they reported an increase of 23%, 48.8% and 61.2% for 25% pumice ratio, 9.2%, 40.7% and 50.3% for 50% pumice ratio 16.3%, 36.1% and 58.8% for 75%pumice ratio, and 12.6%, 36.1% and 58% for 100% pumice ratio respectively. Splitting tensile strength varied between 1.17 MPa to 3.31 MPa respectively.

In the third study [37] with the increase of fiber volume fraction from 0% to 1%, tensile strength increased from 1.9 MPa to 4.1 MPa. Splitting tensile strengths improved 47% to 116% for steel fiber content increase by 0.5% to 1.0%.

2.4.3. Flexural Strength and Behavior of Pumice LWASFRC

In the first study [35], they observed an increase of flexural strength from 4.07 MPa to 5.82 MPa with the increase of steel fiber content from 0% to 2% and improvement in flexural strength was 7% and 42% respectively. They reported that with plain concrete beams brittle failure occurred whereas with increasing fiber content high values of post-peak stress were observed.

In the second study [36], they reported that increase in steel fiber ratio by 0.5%, 1.0% and 1.5% resulted an increase of flexural strength about 37.6%, 79.1% and 120.2% for 25% pumice ratio, 26.3%, 63.1% and 96.8% for 50 pumice ratio, 16.4%, 53.3% and 74.8% for 75% pumice ratio, and 21.9%, 62.1% and 81.1% for 100% pumice ratio respectively.

They reported that flexural strength of the specimens varied between 1.65 to 5.62 MPa for different steel fiber and pumice ratios respectively. They also observed a ductile behavior in specimens with fibers whereas for plain concrete when the peak stress was reached failure occurred suddenly.

In the third study [37], they found flexural strengths up to 2.1, 3.5 and 6.3 MPa for steel fiber contents of 0%, 0.5% and 1% respectively. They reported that flexural energy of specimens were 6.9, 28.9 and 52.2 KN mm for increasing steel fiber content It is obvious that incorporating steel fibers in the mixtures results ductile behavior for concrete.

3. MATERIALS AND METHODS

In this chapter, I will introduce the materials through their mechanical properties, production and testing methods and the machinery that has been used in this work. Chapter 3 consists five topics in it; starting with “Materials” and followed by “Mix Proportions”, “Specimens’ Preparation”, “Test Machines” and “Testing Procedures”.

3.1. Materials

Throughout this work 7 different types of materials used; namely cement, silica fume, fine and coarse aggregates (sand, gravel and pumice), steel fibers, superplasticizer and also standard tap water were used for the production of steel fiber reinforced pumice lightweight aggregate concrete.

3.1.1. Cement

As one of the binders of lightweight aggregate concrete CEM IV/B (P-W) 32.5R type of cement used which was provided by National Technical University of Athens Materials Laboratory.

3.1.2. Silica Fume

Along with cement, small amount of silica fume was also utilized in the mixtures for production of lightweight aggregate concrete. SikaFume®-HR was used. Chemical composition and some physical properties of SikaFume®-HR can be found in Table 3.1 and Table 3.2.

Table 3.1. Chemical Composition of Silica fume (%)

Composition	
SiO_2	96.40
Al_2O_3	0.75
Fe_2O_3	0.56
CaO	0.35
K_2O	0.43
Na_2O	0.04
SO_3	0.05
L.O.I.	3.01

Table 3.2. Physical Properties of Silica Fume

Particle Size (typical)	$< 1\mu m$
Bulk Density (densified)	480 to 720 kg/m^3
Specific Gravity	2.2
Specific Surface	15,000 to 30,000 m^2/kg

3.1.3. Aggregates

Natural type of sand used for this study as fine aggregate with the varying size between 0 to 4 mm. Crushed gravel aggregates were utilized having the size between 4 to 8 mm. Pumice type of lightweight aggregates used with the size varying between 8 – 16 mm. All the aggregate types (Table 3.3) were provided from National Technical University of Athens Materials Laboratory.

Table 3.3. Properties of Aggregates

Aggregates		Unit Weight (g/cm^3)	Water Absorption (% by weight)
Fine Aggregates	Natural Sand	2.63	2.13
Coarse Aggregates	Crushed Gravel	2.67	0.90
	Pumice	1.13	29.00

3.1.4. Fibers

Three different types of hook-end steel fibers used for this study to improve mechanical properties of lightweight aggregate concrete. The properties of steel fibers illustrated in Table 3.4. SF stands for steel fiber whereas the number in parenthesis denotes the length of the fiber. So for example, SF30 denotes for steel fiber with 30mm length. Tensile strength of SF36 and SF60 are not available. Though it is known that those two (SF36 and SF60) types of fibers are made from the same material that of SF30. The length difference may be relevant if we are to consider failure behavior of short and long fibers where, short fibers tend to break whereas long fibers have slipping type of failure.

Table 3.4. Properties of Steel Fibers

	SF30	SF36	SF60
Deformation Type	Hook-end	Hook-end	Hook-end
Length (mm)	30	36	60
Diameter (mm)	0.55	0.63	0.92
Aspect Ratio	55	57	65
Tensile Strength (N/mm^2)	1345	n/a	n/a

3.1.5. Superplasticizer

Sika-Viscocrete® superplasticizer used in this study to improve workability of the concrete in order to compensate negative effects of utilizing steel fibers on the flowability of paste.

3.2. Mix Proportions and Casting

Selected mix proportions and casting procedure is discussed in detail. Sampling and grading analysis of aggregates (natural sand, crushed gravel and pumice) are presented.

3.2.1. Aggregate Grading

Sampling of all types of aggregates has been done according to ASTM D75 [38]. After sampling, sieve analysis conducted according to ASTM C136 [39]. Results of sieve analysis illustrated in Table 3.5

Table 3.5. Sieve Analysis of Aggregates

Sieve Size (mm)	Total Percentage Passing (%)		
	Sand	Gravel	Pumice
16	100	100	100
12.7	100	97.83	87.87
9.51	100	57.13	45.28
6.35	100	6.12	25
4.76	100	0.5	10.13
2.38	75	0	8.23
2	69.5	0	8
1	46.9	0	0
0.5	31.12	0	0
0.25	20.17	0	0

After the sieve analysis and several test productions, aggregate proportions were chosen to be 50% for sand, 15% for crushed gravel and 35% for pumice by total weight of aggregates. (35% for sand, 10% for crushed gravel and 55% for pumice by total aggregate volume). Grading curve for aggregates are presented in Figure 3.1 with respect to reference curves proposed by Fuller and Thomson [40].

After the sampling and sieve analysis, natural sand, crushed gravel and pumice have been heated for 48 hours in a drying oven at 100-105 °C temperature before production to reach oven dry (OD) status.

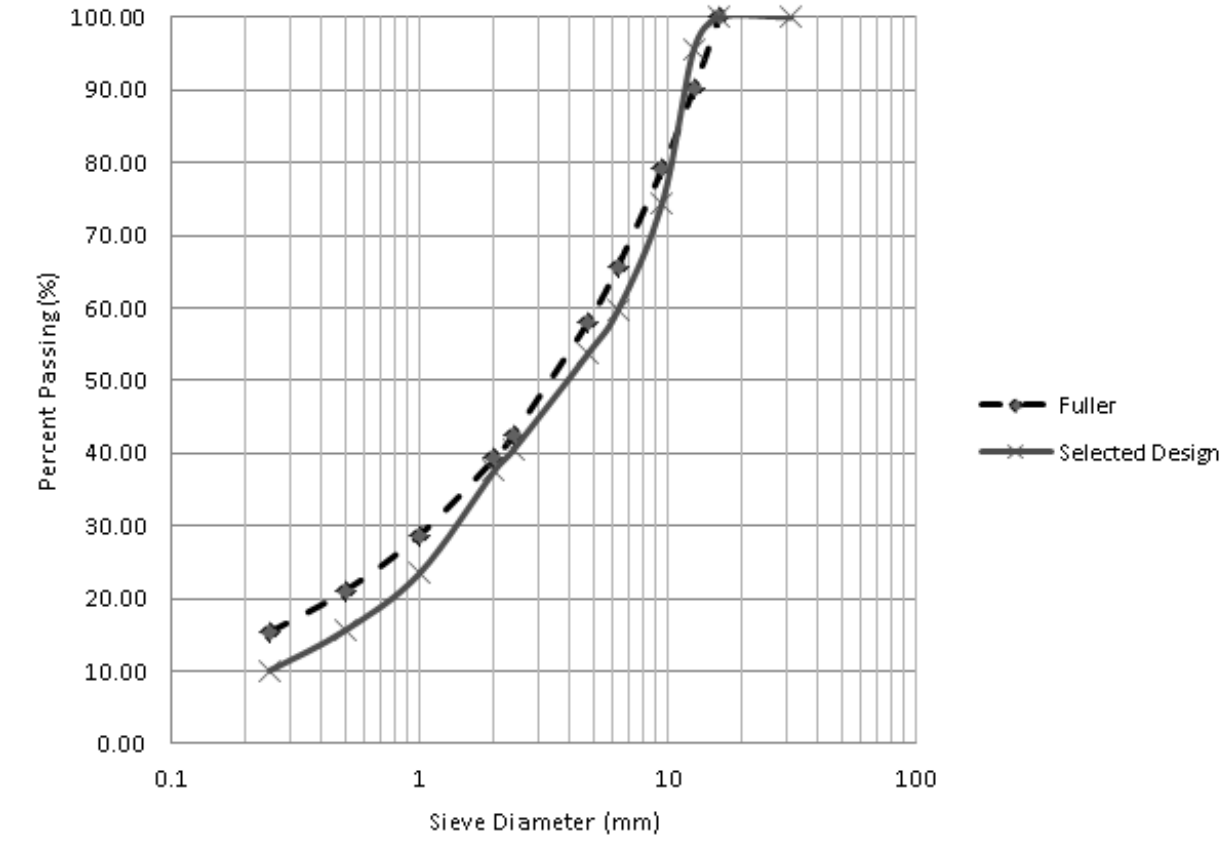

Figure 3.1. Aggregate Grading

3.2.2. Mixture Design

The experimental study contains seven production of pumice LWA steel fiber reinforced concrete, one of them being plain and six other productions for different aspect ratios and volume fractions of steel fibers. Throughout the study, a constant 400kg/m^3 of binder (Portland cement and silica fume) and 227.63 kg/m^3 of water for each mixture resulting 0.40 effective water-cement ratio (w/c) was used. Pumice LWA ratio was constant of 55% of volume fractions of the aggregates, whereas steel fibers are used at two different volume fractions of 0.5% and 1% respectively for each type of aspect ratio of 55, 57 and 65. Superplasticizer utilized with different amounts to have desired workability. Details of mix proportions are presented in Table 3.6.

3.3. Casting and Specimens' Preparation

Before each production, the mixer pallets and tank was wiped with a wet linen cloth in order to prevent loss of water from mixture. Then, relevant amount of LWA was put in the tank and filled with 1/3 of mixture water and kept for 30 mins. After saturation, dry ingredients of mixture were mixed for 5 minutes. Process followed by adding rest of the mixture water. Super-plasticizer was added gradually and mixing process ended with introducing steel fibers after sufficient workability is observed. Laboratory type 50 dm^3 mixer was used for the production of concrete.

3.3.1. Specimens' Preparation

Two different types of molds used throughout the research. For bending tests 100x100x500mm prisms and for compression tests, Poisson's ratio/modulus of elasticity and Barcelona tests Φ150x300mm cylinders were oiled and prepared for casting. Preparation of molds, casting and vibration was done according to ASTM C192/C192M [41].

Table type of vibrator was used for vibration process. Casting was done with different amount of layers and sequences as the standard suggests. After casting, the surface was stroke off with a trowel for finishing. This process continued by moving molds to a plane surface which was chosen close to table vibrator to avoid deficiencies due to carrying of specimens.

Table 3.6. Mix Proportions ($^{kg}/_{m^3}$) – SP: Superplasticizer

	Cement	Silica Fume	Water	w/c (%)	Sand (0 – 4 mm)	Gravel (4 – 8 mm)	Pumice (8 – 16 mm)	Fibers	SP
LC	380	20	227.6	40	600	175	415	0	2.14
LCSF30-0.5	380	20	227.6	40	600	175	415	40	5.12
LCSF30-1	380	20	227.6	40	600	175	415	80	6.44
LCSF36-0.5	380	20	227.6	40	600	175	415	40	4.98
LCSF36-1	380	20	227.6	40	600	175	415	80	5.23
LCSF60-0.5	380	20	227.6	40	600	175	415	40	5.00
LCSF60-1	380	20	227.6	40	600	175	415	80	5.28

LC: Lightweight Concrete, SF: Steel fiber, Length of Fibers, Volume fraction of Fibers

The specimens covered with a sack type of material after production which was moisturized for 24 hours in an interior space with room temperature until demolding. After demolding, specimens were carried in a curing pool with 20±2 °C water temperature (Figure 3.2). Curing lasted until 28 days for each production.

Figure 3.2. Specimens in the curing pool

3.3.2. Capping

A capping procedure was needed for cylindrical specimens for uniform stress distribution for compression and Poisson's ratio/modulus of elasticity tests since the top side of the molds are open air which results non-smooth surfaces considering also the effect of bleeding phenomenon. Capping procedure was not applied to Barcelona test specimens. This will be explained in following paragraphs.

Capping was done at 21st day of curing. The cylindrical specimens were first taken from the curing pool to a flat surface. Then the head parts of the specimens were covered circumferentially with a thin film around 1-2 mm higher than the surface of the specimens which then stabilized with a steel bracelet and checked for the leveling with spirit and bull's eye leveling tools.

Procedure continued with preparation of repairing type fibered cement paste with very low w/c ratio. After enough workability was observed, the paste casted on top of the specimens with the help of a trowel. For ease of casting, trowels were wetted throughout the procedure. Leveling was checked once again after finishing the surface; later on, specimens were covered with a wet sack type of cloth and kept 24 hours in room temperature. After 24 hours, specimens were taken back to the curing pool for finishing the curing procedure.

3.3.3. Preparation of Barcelona Test Specimens

After 28 days of curing, specimens were taken out of the curing pool and carried to the testing laboratory. As it is already mentioned, during the casting of Barcelona test specimens Φ150x300 mm cylindrical molds were used. Yet according to standard procedure of this test Φ150x150 mm specimens are needed. Since it is not practical to cast concrete in these dimensions, in lengthy molds; Barcelona test specimens were casted around 180 – 190 mm height. These specimens later on cut by a crystal sawing machine at 150 mm height before testing. Since the cutting operation results smooth surfaces for Barcelona test specimens, capping was not needed.

One of the important things to consider while cutting specimens is to get flat top surfaces. In the case that the surface is not flat, this can create eccentricity in the behavior of the specimens while loading.

3.4. Testing Machines

Console system and machines were produced by an Italian brand CONTROLS. The specific product ADVANTEST 9, servo-hydraulic control console with a compression loading frame of 5000 kN capacity was used for the load control compression tests. A flexural frame of 150 kN capacity was used for displacement control bending tests which was driven by the same console unit.

3.5. Testing Procedures

All of the tests carried out in the materials engineering testing laboratory of National Technical University of Athens. In the following sub-topics detailed explanations of testing procedures and standards will be explained.

3.5.1. Tests and Calculations for Fresh State Properties

3.5.1.1. Slump Test. After the production process slump tests were conducted according to ASTM C143 [42]. A slump cone filled with fresh concrete in three layers and each layer was hit 25 strokes with a rod to release air for better compacting of concrete. After filling procedure, top layer of concrete was stroke off with a trowel and then cone was released. Distance between top of the cone and slightly consolidated concrete pile measured.

3.5.1.2. Density Test and Air Content Measurement. A bucket with dimensions of Φ150x200mm filled and vibrated with two equal layers according to ASTM C138/C138M for density test [43]. The surface of the concrete was finished with a trowel and bucket was cleaned from excessive concrete to not to bias the measurement. Density of each specimen calculated considering the weight and volume of the bucket used.

Air content calculated according to following equation:

$$A = [\frac{(T-D)}{T}] \times 100 \quad (3.1)$$

Where A is air content by percentage, T is calculated theoretical concrete density(kg/m^3), D is measured concrete density(kg/m^3).

3.5.2. Tests for Hardened State Properties

3.5.2.1. Compressive Strength, Modulus of Elasticity and Poisson's Ratio. Compressive strength tests were performed according to ASTM C39/C39M for cylindrical specimens (Figure 3.3) [44]. Compression tests continued until clear fracture patterns observed. After reaching ultimate load, the machine has been unloaded and specimens carried away for further observations.

Modulus of elasticity and Poisson's ratio tests were conducted according ASTM C 469 – 02 [45]. Transverse strain was recorded with the help of a linear variable differential transformer (LVDT) attached at the mid-height of the specimen. Before each test LVDT's performance (if It is set or not) was checked. Tests carried on in two phases. At the first phase, specimens loaded until the 40% of ultimate strength and then load released until 5% of the ultimate strength in three cycles. After the last cycle specimen loaded until total failure. Finally specimens carried away for further investigation.

Figure 3.3. Test Setup for Compressive Strength, Modulus of Elasticity and Poisson's Ratio

3.5.2.2. 3 Point Bending Test with notched beams. 3 point bending tests were conducted on prism specimens with 100x500x500mm dimension (Figure 3.4.). One of the most prominent effects of fiber addition to concrete is their positive contribution to ductility. Hence fracture parameters such as toughness (energy absorption) and fracture energy were calculated. Limit of proportionality and flexural strength (modulus of rupture) values were also evaluated. BS EN 14651 + A1:2007 was the standard followed for calculation of these values [46].

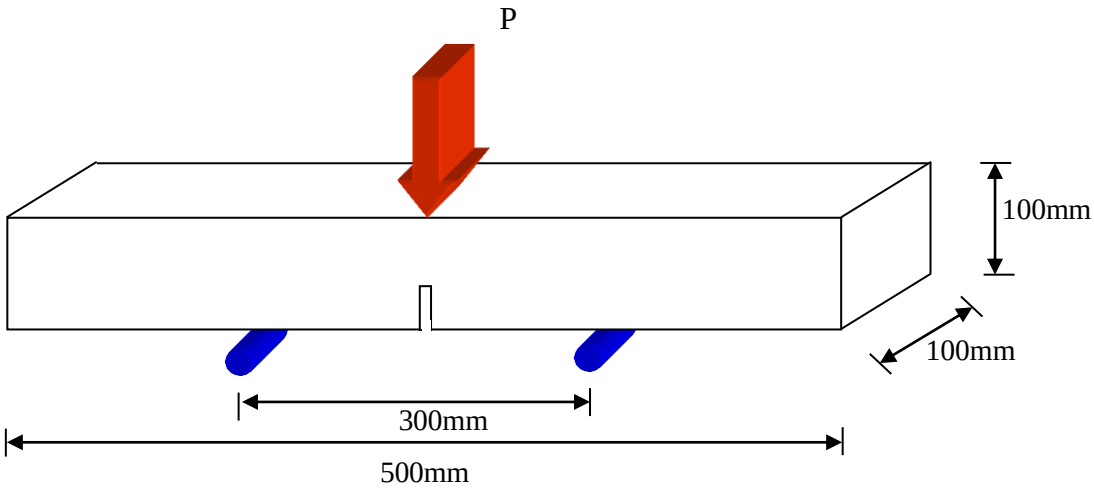

Figure 3.4. 3 point bending test setup

Test setup for 3 point bending test presented at Figure 3.3. After the production of prism specimens a notch with 4 mm width and 16±1 mm height was cut with a crystal sawing machine. In order to measure crack mouth opening displacement (CMOD), a metal apparatus glued at the crack tip with 5 mm height and an extensometer attached horizontally prior to every test procedure (Figure 3.5).

Figure 3.5. Attached metal apparatus and test setup

All the calculation for limit of proportionality and flexural strength was done according to aforementioned standard. Toughness (energy absorption) was calculated by the area under load-displacement curve. Fracture energy, G_F (N/m), is given in equation 3.2 as;

$$G_F = \frac{W_0 + m\frac{S}{U}g\delta_0}{A_{eff.}} \tag{3.2}$$

Where W_0 is toughness (N*mm), m is weight of the beam (kg), g is gravitational constant ($m^3 \cdot kg^{-1} \cdot s^{-2}$), S and U are span and length of the beam (mm), δ_0 is final deflection (mm), $A_{eff.}$ is effective cross-section ($m^{2)}$.

3.5.2.3. Barcelona Test. In this study also Barcelona test (double-punch test) was done in order to obtain tensile and fracture behavior of specimens. Both standard Barcelona test provided by UNE 83-515 and Generalized Barcelona (G-BCN) test proposed by Carmona *et al.* was conducted [47][48].

The test is conducted by placing 2 metal wedges between loading platen and cylindrical specimens with Φ150x150mm dimensions. The radius of metal wedges is 37.5 mm. Measurement is done by placing 3 LVDT's at loading platen with 120° to each other and a circumferential extensometer placed with the help of a chain which is placed at the middle of the specimens. The loading rate kept constant of 0.5mm/min throughout the test. Applied load, vertical and circumferential displacements are recorded until the total failure (Figure 3.6).

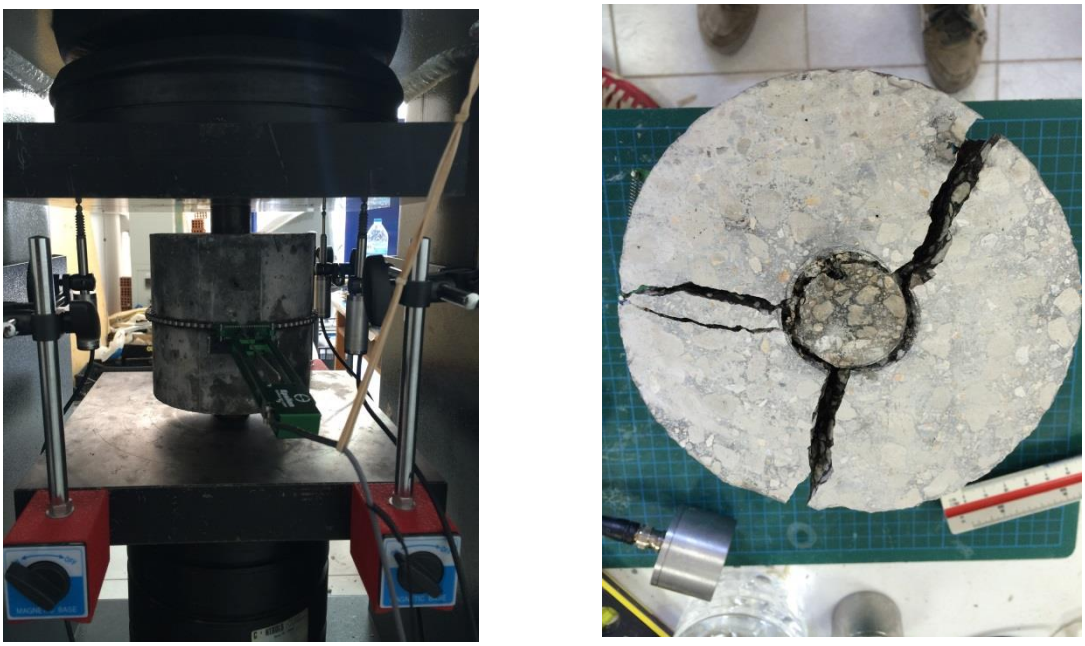

Figure 3.6. Test setup and a broken Barcelona test specimen

Circumferential extensometer readings provide total circumferential opening displacement (TCOD) where area under Load-TCOD curve is defined as energy absorption of concrete E(TCOD) as it is presented in Equation 3.3

$$E(TCOD) = \int_0^{TCOD} P(TCOD)d(TCOD) \quad (3.3)$$

For G-BCN test instead of TCOD, axial displacements are taken into consideration. Toughness of the specimens is calculated by the area of Load-axial displacement curves as it is presented in Equation 3.4.

$$T(\delta_A) = \int_0^{\delta_A} P(\delta) d(\delta) \tag{3.4}$$

Standard UNE 85-515 defines f_{ct} first peak strengths which are calculated by P_f peak loads as it is presented in Equation 3.5.

$$f_{ctRx} = \frac{4P_{Rx}}{9\pi ah} \tag{3.5}$$

Where 2a is the diameter and 2h is the height of metal wedge. For both Barcelona and G-BCN tests TCOD and axial displacements are taken in post-cracking phase at 1.5mm, 2.5mm and 3.5mm values.

4. RESULTS AND DISCUSSIONS

In this chapter fresh and hardened state results of concrete will be discussed in detail.

4.1. Fresh State Properties of Concrete

4.1.1. Unit Weight, Slump and Air Content

According to unit weight tests, all the specimens have unit weight lower than 2000 kg/m^3 which is the limit value for concretes to be defined as lightweight concrete. According to BS-EN 206, Plain LC and LCSF36-1 are in class S2 (Slump 50 to 90 mm), LCSF30-0.5, LCSF60-0.5 and LCSF60-1 are in class S3 (Slump 100 to 150 mm) and LCSF30-1 is in class S4 (160 to 210 mm). LCSF30-1 has a very high slump value compared to other mixtures. Unit weight and slump values are presented in Table 4.1 for each mixture [49].

Table 4.1. Unit weight and Slump Values

	LC	LCSF30-0.5	LCSF30-1	LCSF36-0.5	LCSF36-1	LCSF60-0.5	LCSF60-1
Unit Weight (kg/m^3)	1,775	1,803	1,805	1,832	1,841	1,829	1,807
Slump (mm)	50	120	190	90	60	100	100
Air content (%)	2.53	3.17	5.15	1.61	3.26	1.77	4.99

4.2. Hardened State Properties of Concrete

4.2.1. Compressive Strength

Results for compressive strength of each specimen presented at Table 4.2. Plain concrete specimens had 17.68, 20.07 and 17.92 MPa compressive strength with the average compressive strength of 18.55 MPa. Considering the average compressive strength values, there was 16.1% and 43.2% increase for 0.5% and 1% fiber fractions for LCSF30 respectively. Whereas for LCSF36 the increase was 31.7% and 69% and for LCSF60 20.8% and 76.3% for 0.5% and 1% volume fractions respectively.

Table 4.2. Compressive Strength of Each specimen (MPa)

	A	B	C	Avg.	Std.	CV(%)
LC	17.68	20.07	17.92	18.55	1.31	7.09
LCE	29.55	31.66	31.8	31.00	1.26	8.57
LCSF30-0.5	19.71	22.83	22.08	21.54	1.62	7.56
LCSF30-1	22.27	28.65	28.79	26.57	3.72	14.01
LCSF36-0.5	20.17	27.09	26.08	24.44	3.73	15.29
LCSF36-1	31.15	32.98	29.94	31.35	1.53	4.88
LCSF60-0.5	22.64	20.74	23.87	22.41	1.57	7.03
LCSF60-1	31.27	31.07	35.79	32.71	2.66	8.16

Due to the high variation of compressive strength values a new mix was prepared with the same mix design that of LC. The new specimen named LCE (E denotes for extra) which the top surface was grinded instead of capping. The new specimens have 31.00 MPa average compressive strength. Compared to LC with 18.55 MPa average compressive strength, it can be said that application of thin mortar layer as capping results 40% decrease in compressive strength results. Values for other specimens can be interpreted also from this perspective.

The results for each set of specimens are homogenous with 8.57% coefficient of variation at most. The exceptions are LCSF30-1 and LCSF36-0.5 with 14.01% and 15.29% coefficient of variation respectively. This deviation may be due to the possibility of obtaining maximum and minimum values where 3 specimen sample size was used. The lowest compressive strength value obtained for LC and the high compressive strength value obtain for LCSF60-1. Considering the other results, inconsistent effect of fiber addition was observed. Either the improvement is neglectable (LCSF30-1 and LCSF60-0.5 compared to LC) or higher than 50% (LCSF36-1 and LCSF60-1 compared to LC). Similar minimal effect [36] or inconsistent effect [35.,37] of fiber addition were found also in the literature. Average compressive strength values for all specimens presented at Figure 4.1.

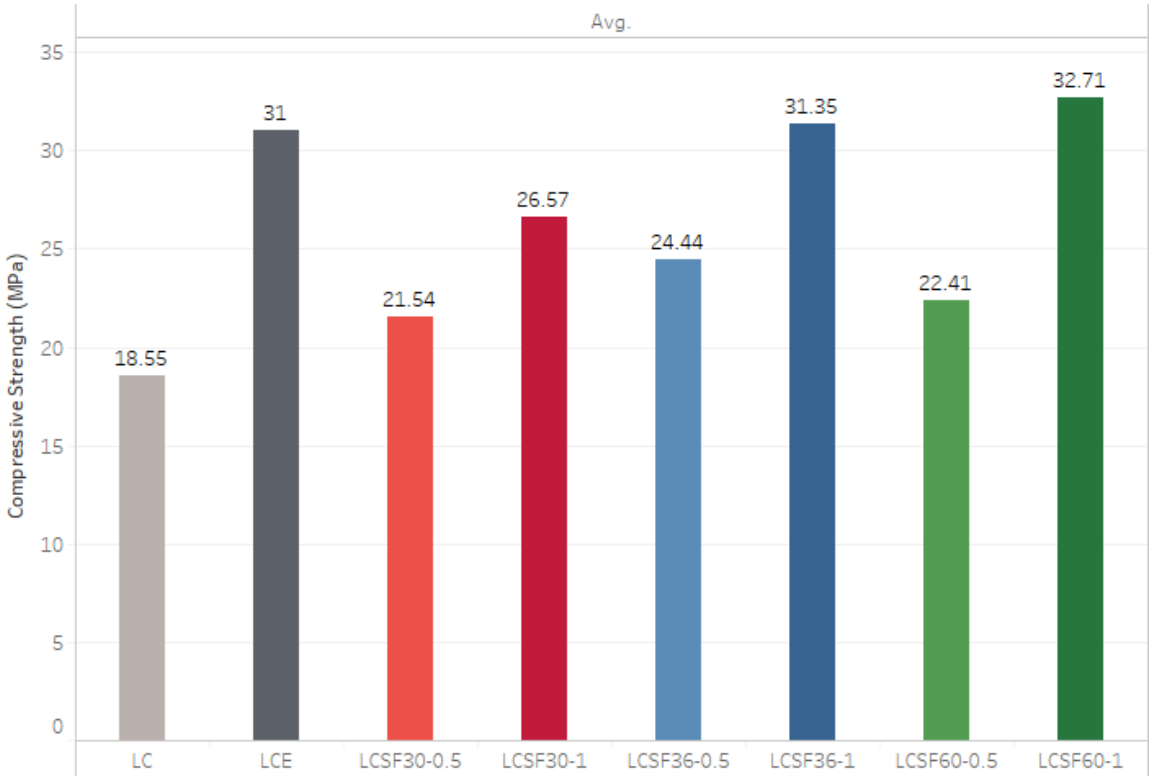

Figure 4.1. Average compressive strength values for each mixture

4.2.2. Elasticity Modulus and Poisson's Ratio

The Results of modulus of elasticity for each specimen, average modulus of elasticity values, standard deviation and coefficient of variation are presented at Table 4.3. All compositions have relatively common values for modulus of elasticity. It can be concluded that the effect of fiber addition until 40% compressive strength value has no significant effect.

Table 4.3. Modulus of elasticity of each specimen (GPa)

	A	B	C	Avg.	Std.	CV(%)
LC	17.17	20.17	16.91	18.09	1.81	10.01
LCE	15.93	18.3	19.12	17.78	1.65	9.3
LCSF30-0.5	19.25	15.64	20.11	18.33	2.4	13.01
LCSF30-1	17.75	17.99	16.5	17.41	0.8	4.6
LCSF36-0.5	22.81	17.72	17.82	19.45	2.9	14.95
LCSF36-1	19.78	20.05	18.29	19.37	0.95	4.9
LCSF60-0.5	18.81	17.67	18.38	18.29	0.58	3.17
LCSF60-1	18.5	18.38	18.88	18.59	0.25	1.39

Most of the productions have 10% coefficient of variation with the exceptions of LCSF30-0.5 and LCSF36-0.5. Considering the compressive strength values, high coefficient of variation was observed for LCSF36-0.5 where for LCSF30-0.5 had low coefficient of variation. Considering both LCSF36-0.5 and LCSF36-1 with highest modulus of elasticity values were also the heaviest 2 specimens as presented above.

The volume fraction of fibers seems to have no effect on modulus of elasticity values since results are very similar for each set of compositions (LCSF30, LCSF36 and LCSF60). Comparing LC and LCE the difference between modulus of elasticity values are very low, suggesting that grinding the top of surface had no effect compared to capping application at 40% of compressive strength for each set of specimens. The average values for modulus of elasticity are presented at Figure 4.2.

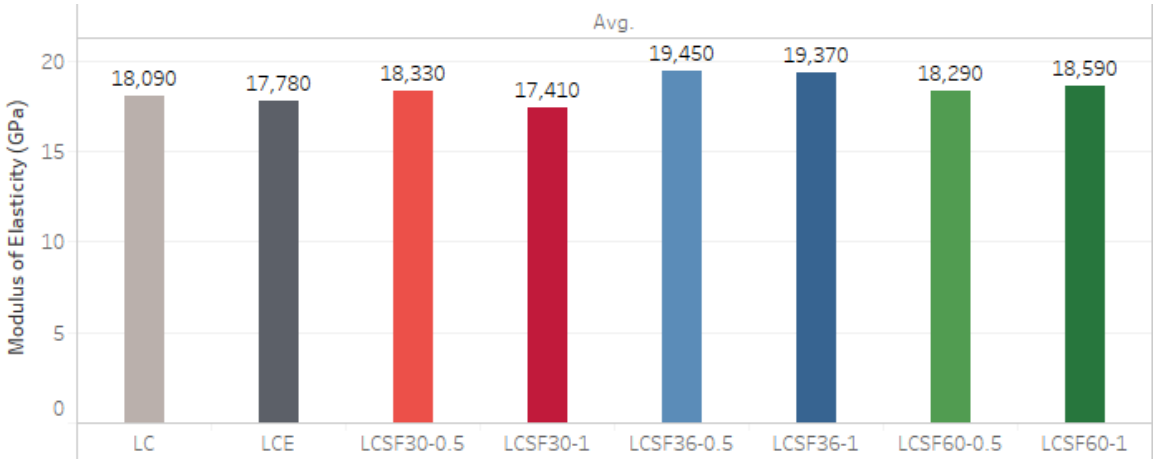

Figure 4.2. Average values of Modulus of elasticity

Results for Poisson's ratio, average value, standard deviation and coefficient of variations are presented at Table 4.4. Results for LC, LCE and LCSF30-0.5 are heterogeneous whereas for other set specimens they are relatively homogenous. The peak values were observed with LC and LCSF36-1 compositions. Due to a test fallacy, results for LC A specimen cannot be presented. Average values for specimens are presented at Figure 4.3.

Table 4.4. Poisson's Ratio Values

	A	B	C	Avg.	Std.	CV(%)
LC		0.26	0.22	0.24	0.028	11.67
LCE	0.18	0.23	0.25	0.22	0.036	16.36
LCSF30-0.5	0.25	0.19	0.21	0.22	0.031	14.31
LCSF30-1	0.22	0.23	0.21	0.22	0.01	4.55
LCSF36-0.5	0.24	0.22	0.23	0.23	0.01	4.35
LCSF36-1	0.26	0.25	0.21	0.24	0.026	10.83
LCSF60-0.5	0.20	0.23	0.22	0.22	0.015	6.92
LCSF60-1	0.22	0.22	0.23	0.22	0.006	2.69

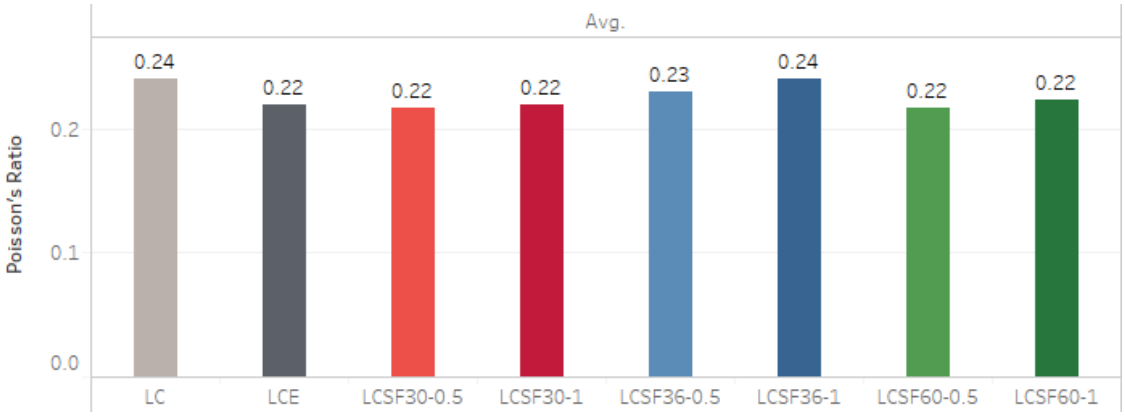

Figure 4.3. Average values for Poisson's ratio

4.2.3. 3 Point Bending Test

Results for f_{LOP} , average values, standard deviation and coefficient of variation are presented at Table 4.5 (The results for LC C specimen cannot be presented due to a test fallacy.). Plain concrete LC has the lower value of f_{LOP} , where increase of fiber volume fraction and aspect ratio increased f_{LOP} as it is expected.

Table 4.5. f_{LOP} values for each specimen (MPa)

	A	B	C	Avg.	Std.	CV(%)
LC	3.19	2.91		3.05	0.198	6.50
LCSF30-0.5	4.44	4.16	4.20	4.27	0.151	3.50
LCSF30-1	4.87	4.51	5.10	4.83	0.297	6.20
LCSF36-0.5	3.98	4.45	3.90	4.11	0.297	7.20
LCSF36-1	4.64	6.42	4.88	5.31	0.966	18.18
LCSF60-0.5	4.28	4.04	4.51	4.28	0.235	5.50
LCSF60-1	5.86	6.07	6.33	6.09	0.235	3.87

Almost all the values show high homogeneity except LCSF36-1. LC60-1 has the highest value of 6.09 MPa where LCF30-0.5 has the lowest value of 4.27 among the composition with fibers. Average values for f_{LOP} are present at Figure 4.4.

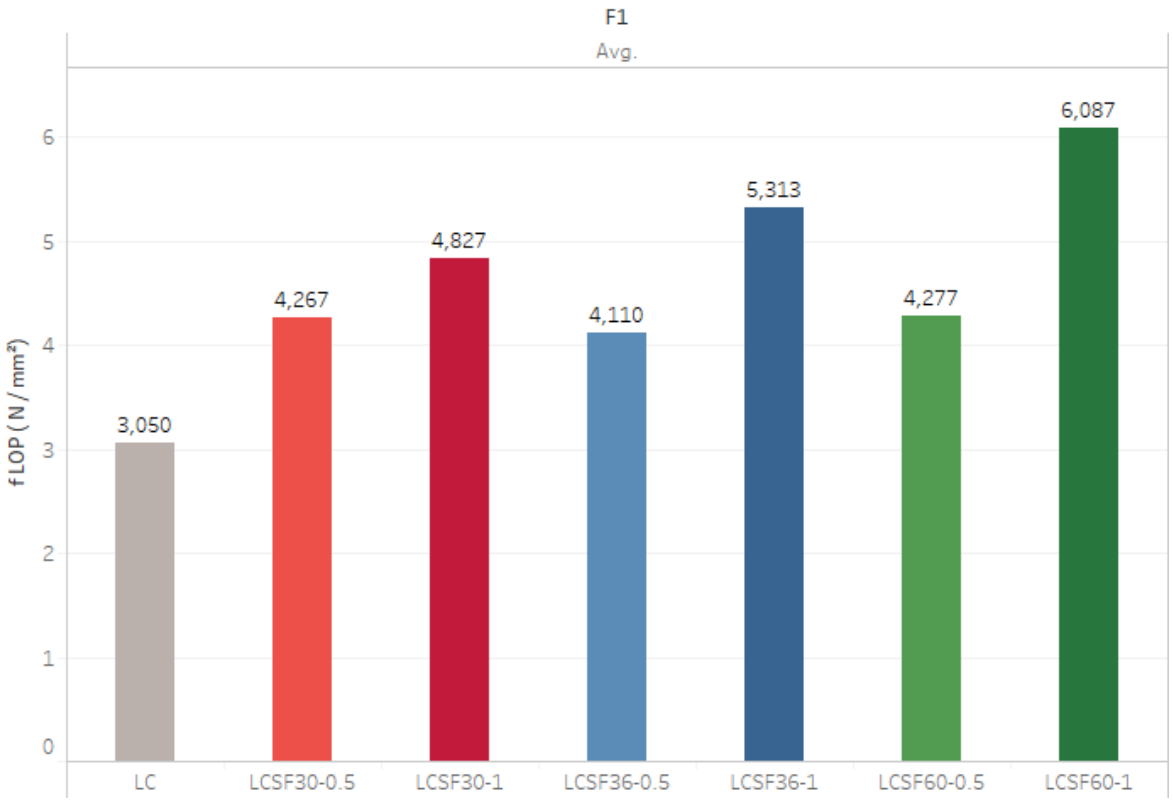

Figure 4.4. Average values of f_{LOP} for each mixture (MPa)

Results for flexural strength (modulus of rupture), average values, standard deviation and coefficient of variation are presented at Table 4.6. Results are mostly homogenous with the exception of LCSF60-0.5 where coefficient of variation is 13.74%. Highest value is 10.33 MPa for LCSF60-1, where lowest value is 3.05 MPa for LC as it is expected.

Table 4.6. Results of Flexural Strength for each specimen (MPa)

	A	B	C	Avg.	Std.	CV(%)
LC	3.19	2.91		3.05	0.198	6.49
LCSF30-0.5	4.44	4.16	4.2	4.27	0.151	3.55
LCSF30-1	4.87	4.79	5.1	4.92	0.161	3.27
LCSF36-0.5	5.49	5.09	6.18	5.59	0.551	9.87
LCSF36-1	8.93	10.12	8.21	9.09	0.965	10.61
LCSF60-0.5	5.92	7.66	6.32	6.63	0.911	13.74
LCSF60-1	9.21	10.54	10.33	10.03	0.715	7.13

The difference between high volume fraction of fibers (1%) and low volume fraction of fibers (0.5%) are evident. It is obvious that the increase in fiber content results high flexural strengths as it is expected. LCSF36-1 has 9.09 MPa flexural strength where LCSF60-0.5 has 6.63 MPa flexural strength. It can be asserted that fiber content has higher effect on flexural strength than aspect ratio of fibers.

The values for LC and LCSF30-0.5 are the same of f_{LOP} values. It suggests these compositions have softening behavior. Also for LC30-1 A and LC30-1 C we can observe same results between f_{LOP} and flexural strength. LC30-1 B has relatively higher flexural strength value. For all the rest of the specimens, flexural strengths exceed f_{LOP} values, suggesting hardening behavior. It can be seen in Appendix A that LCSF30-0.5 and LCSF30-1 mixtures have softening behavior whereas varying hardening behavior was observed for the rest of the specimens except the control group. It can be said that length difference between 36mm and 30 mm steel fibers are critical. As the length of the fibers increase the failure behavior of fibers change from sudden break to slipping. This phenomenon can explain that resulting slip hardening behavior of LCSF36-0.5 composition where even though the volume fraction of fibers is low, strain hardening behavior remains. Average values of flexural strength presented at Figure 4.5.

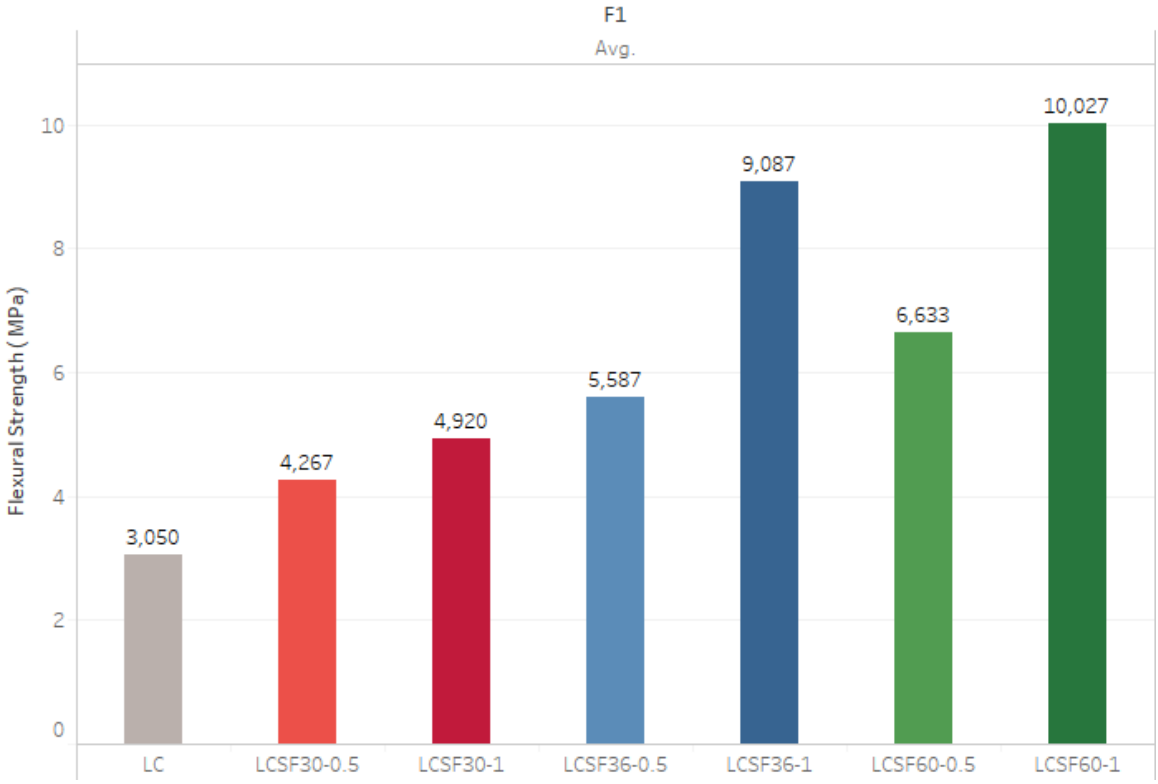

Figure 4.5. Average values of flexural strength (MPa)

One of the most prominent parameter is toughness when bending tests with fiber reinforced composites are considered. The area under load-CMOD curve gives toughness (energy absorption) values. At Table 4.7, results for toughness, average value, standard deviation and coefficient of variation are presented until 3.5mm deflection. LCSF30-0.5 has very high coefficient of variation value which exceeds 24%. Whereas LCSF36-1 has 19% coefficient of variation and LCSF60-0.5 has 16% coefficient of variation. This high variation can be explained by the nature of bending test. After the first crack appears, the propagation of the crack depends on both concentration and distribution of the fibers at the effective cross-section of the specimen beginning from the top of the notch to the top of the specimen.

The peak value is observed with LCSF60-1 which suggests that high aspect ratio results higher ductility. Plain concrete LC had sudden break with almost no ductile behavior as it is expected. It can be said that both aspect ratio and volume fraction of the fibers have significant impact on toughness. Results for average values are presented at Figure 4.6.

Table 4.7. Values of Toughness for each specimen (N*m)

	A	B	C	Avg.	Std.	CV(%)
LC	84	76		80	6	7.07
LCSF30-0.5	16728	10531	12139	13133	3216	24.49
LCSF30-1	19818	21569	17623	19670	1977	10.05
LCSF36-0.5	22630	21351	25005	22995	1854	8.06
LCSF36-1	33936	44714	31538	36729	7018	19.1
LCSF60-0.5	25042	34724	29804	29857	4841	16.21
LCSF60-1	36414	42846	42115	40458	3522	8.7

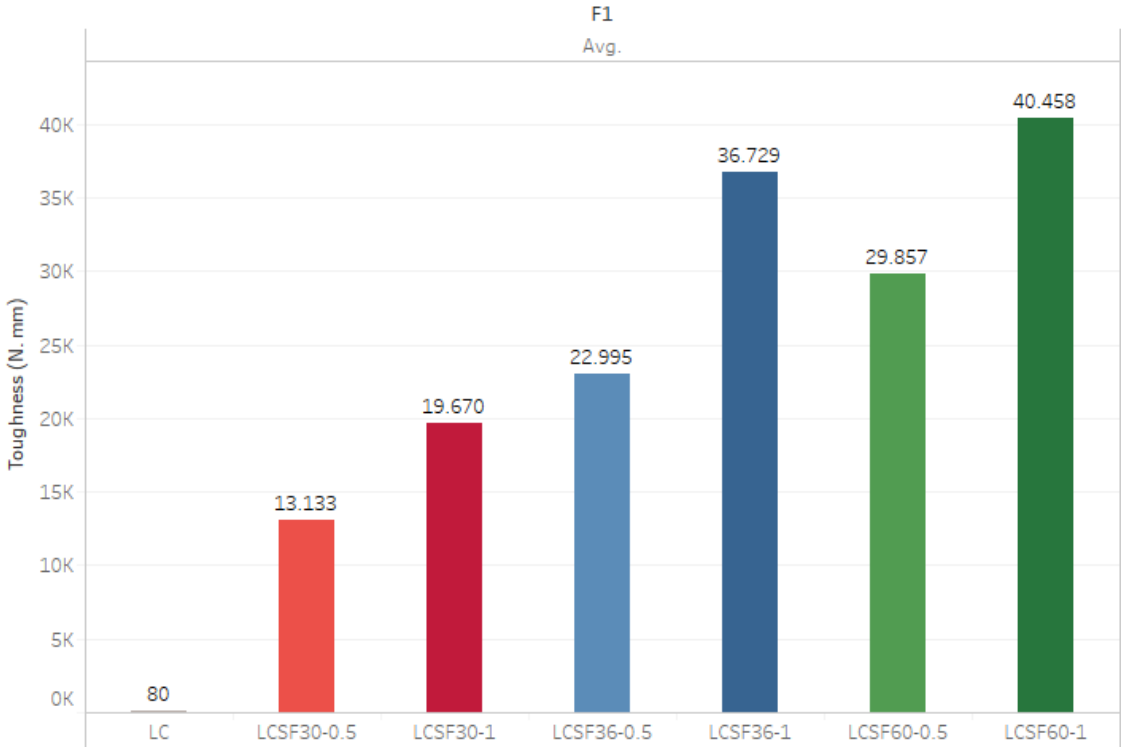

Figure 4.6. Average values of Toughness for each mixture

Fracture energy values are presented at Table 4.8. Results show that high volume fraction of fibers has significant effect on ductile behavior. As the aspect ratio of fibers increase fracture energy is also increased. Similar observations that had been made for toughness can be made here as well.

Table 4.8. Fracture Energy Values (N/m)

	A	B	C	Avg.	Std.	CV(%)
LC	34.0	33.1		33.6	0.7	2
LCSF30-0.5	2063.8	1308	1504.2	1625.3	392.2	24.13
LCSF30-1	2440.6	2627.5	2172.8	2413.6	228.5	9.47
LCSF36-0.5	2783.5	2627.5	3073.1	2828.0	226.1	8.00
LCSF36-1	4126.4	5476.6	3873.2	4492.1	862.0	19.19
LCSF60-0.5	3077.6	4157.1	3658.3	3631.0	540.3	14.88
LCSF60-1	4464.5	5248.9	5159.8	4957.7	429.5	8.66

4.2.4. Barcelona Test Results

Tensile strength results, average values, standard deviation and coefficient of variation for all mixtures are presented in Table 4.9.

Table 4.9. Tensile strength of each specimen (MPa)

	A	B	C	Avg.	Std.	CV(%)
LC	2.39	2.59	2.49	2.49	0.1	4.03
LCSF30-0.5	2.72	2.65	2.44	2.6	0.15	5.75
LCSF30-1	2.59	2.65	2.72	2.65	0.065	2.44
LCSF36-0.5	2.4	2.72	2.45	2.52	0.174	6.9
LCSF36-1	2.63	2.78	2.63	2.68	0.085	3.16
LCSF60-0.5	2.91	2.21	2.74	2.62	0.363	13.85
LCSF60-1	2.52	3.09	2.79	2.8	0.285	10.18

LCSF60-0.5 and LCSF60-1 mixtures have high coefficient of variation whereas with the other mixtures homogenous results are observed. Mixture with no fibers, LC, has the

lowest average tensile strength value of 2.49 MPa where LCSF60-1 has the highest average value of 2.80 MPa. With all the different aspect ratios of fibers, an increase with high volume fraction (1%) compared to low volume fraction (0.5%) is also observed.

Compared to LC, LCSF36-0.5 has nearly the same value of tensile strength. LCSF30-0.5 and LCSF60-0.5 have 2.60 MPa and 2.62 MPa tensile strength values respectively. Considering low fraction of fibers (0.5%) It is not possible to mention a significant effect of fiber addition. This may be due to the nature of the Barcelona test or the fact that 0.5% fiber volume fraction has almost no effect on tensile behavior of specimens since it is a very low amount of fibers. Whereas for 1% volume fraction of fibers, although the effect of fiber addition is low (6% to 12% increase) It is not neglectable. It can be said that increasing aspect ratio of fibers has a greater contribution to tensile behavior of concrete. (Figure 4.7). Results for all the mixtures at 1.5, 2.5 and 3.5mm TCOD are given at Table 4.10. Average values, standard deviation and coefficient of variation values are presented at Table 4.11.

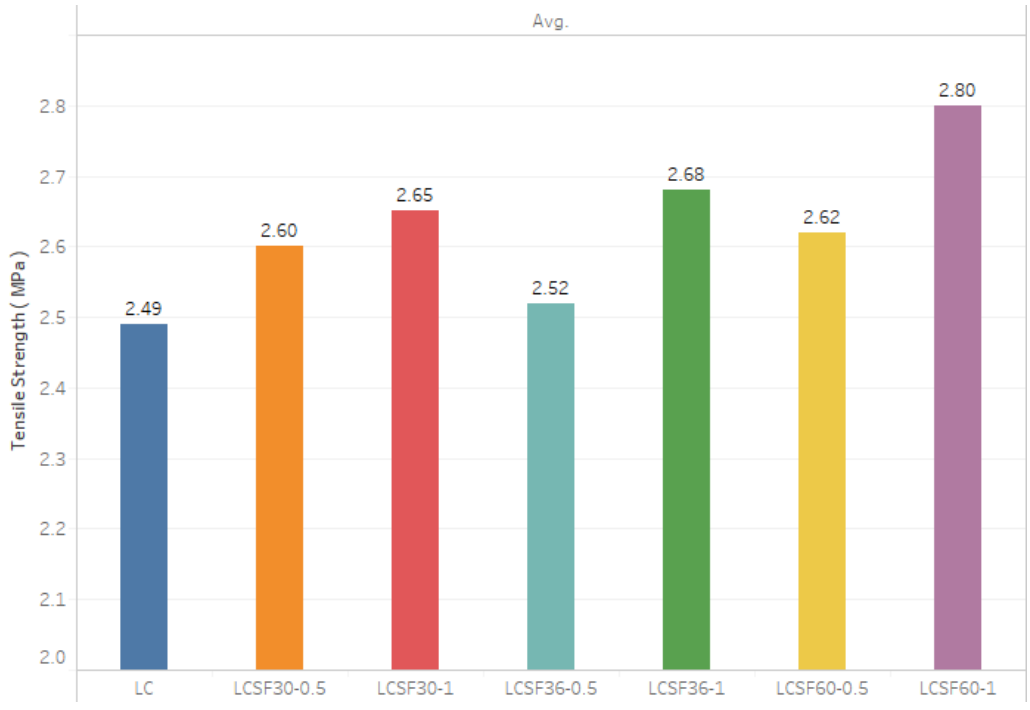

Figure 4.7. Average tensile strength of each mixture (MPa)

Table 4.10. Toughness for different TCOD values (N*m)

	A1500 (μm)	B1500 (μm)	C1500 (μm)	A2500 (μm)	B2500 (μm)	C2500 (μm)	A3500 (μm)	B3500 (μm)	C3500 (μm)
LC	0	0	0	0	0	0	0	0	0
LCSF30-0.5	97.66	88.15	72.25	137.59	121.59	98.45	169.94	147.02	117.9
LCSF30-1	94.84	99.32	119.58	135.37	143.87	181.15	170.19	177.71	229.55
LCSF36-0.5	112.19	98.38	104.1	172.97	139.19	151.91	221.83	170.08	188.12
LCSF36-1	102.63	125.94	125.98	148.79	188.82	191.98	184.73	238.69	245.92
LCSF60-0.5	111.91	83.54	118.37	162.26	127.01	181.25	200.47	167.23	226.76
LCSF60-1	119.19	145.34	126.25	191.71	224.94	194.63	259.36	292.22	251.06

Table 4.11. Average Toughness for different TCOD values and coefficient of variations (N*m)

	Avg. 1500 (μm)	SD 1500 (μm)	CV (%) 1500 (μm)	Avg. 2500 (μm)	SD 2500 (μm)	CV (%) 2500 (μm)	Avg. 3500 (μm)	SD 3500 (μm)	CV (%) 3500 (μm)
LC	0	0	0	0	0	0	0	0	0
LCSF30-0.5	86.02	12.84	14.93	119.24	19.68	16.51	144.98	26.03	17.96
LCSF30-1	104.58	13.19	12.61	153.46	24.35	15.87	192.48	32.32	16.79
LCSF36-0.5	104.89	6.94	6.62	154.69	17.06	11.03	193.34	26.27	13.59
LCSF36-1	118.18	13.47	11.4	176.53	24.08	13.64	223.11	33.43	14.99
LCSF60-0.5	104.61	18.53	17.71	156.84	27.52	17.55	198.15	29.83	15.06
LCSF60-1	130.26	13.53	10.38	203.76	18.4	9.03	267.55	21.76	8.13

Barcelona test considers only the post-cracking behavior of specimens. There was a sudden failure with LC mixture after peak load was reached hence all the values for LC mixture are zero. According to Carmona et. al. [48] one of the advantages of Barcelona test is lesser scattering of the results compared to other fracture tests. Considering coefficient of variation for 3.5mm displacement the maximum coefficient of variation is observed with LCSF30-0.5 (18%). For 3 point bending test maximum coefficient of variation value was 24%.

Average values for TCOD is presented as a bar graph in Figure 4.8. Considering 0.5% volume fraction of fibers, there is a significant improvement between LCSF30 and other two aspect ratios of fibers. However LCSF36 and LCSF60 have similar values. For the former it can be said that above 30mm of fiber length, fibers tend to work better for holding cracks perhaps due to slipping type of failure behavior. For the latter, there seems to be a limiting factor for the improvement of fiber length and/or aspect ratio perhaps due to low volume fraction (0.5%) of the fibers. Whereas significant improvement can be observed for 1% volume fraction of fibers.

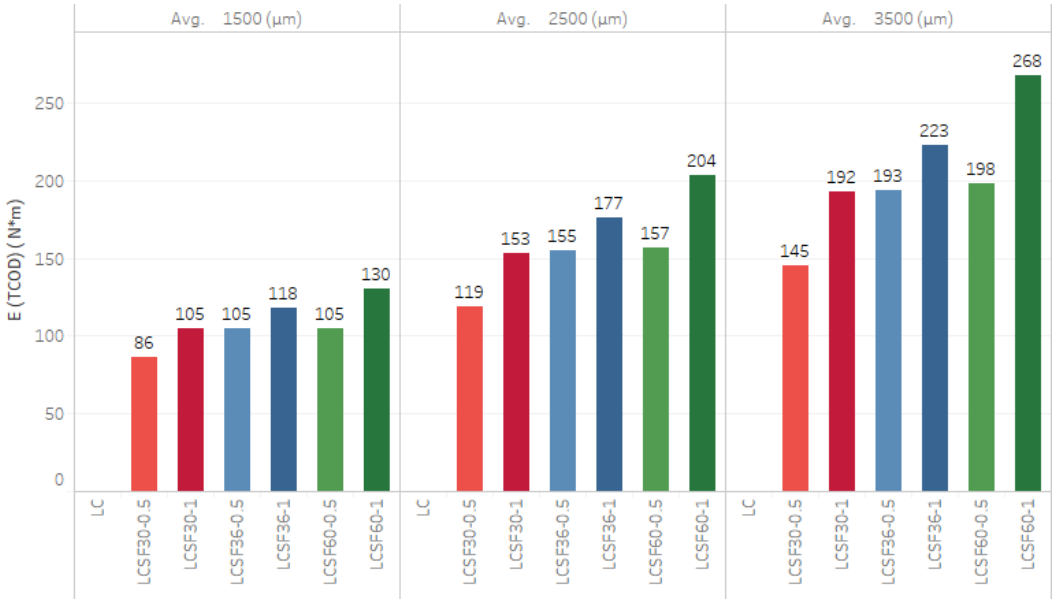

Figure 4.8. Average Toughness values (N*m)

Table 4.12. G-BCN toughness for each specimen at different axial displacement (N*m)

	A1500 (μm)	B1500 (μm)	C1500 (μm)	A2500 (μm)	B2500 (μm)	C2500 (μm)	A3500 (μm)	B3500 (μm)	C3500 (μm)
LC	0	0	0	0	0	0	0	0	0
LCSF30-0.5	48.19	48.55	28.55	84.26	82.24	54.44	113.93	106.93	73.83
LCSF30-1	65.79	63.65	39.24	105.16	111.72	124.07	138.02	147.57	204.16
LCSF36-0.5	14.58	68.61	44.51	93.52	118.1	108.7	165.17	155.07	154.29
LCSF36-1	59.68	26.04	31.12	111.58	117.99	92.13	153.94	201.36	179.03
LCSF60-0.5	62.34	34.53	42.05	106.02	82.87	117.15	142.13	126.31	183.24
LCSF60-1		76.19	80.93		170.1	162.32		256.89	239.74

Table 4.13. G-BCN average toughness values and coefficient of variations (N*m)

	Avg. 1500 (μm)	SD 1500 (μm)	CV (%) 1500 (μm)	Avg. 2500 (μm)	SD 2500 (μm)	CV (%) 2500 (μm)	Avg. 3500 (μm)	SD 3500 (μm)	CV (%) 3500 (μm)
LC	0	0	0	0	0	0	0	0	0
LCSF30-0.5	41.76	11.44	27.39	73.64	16.66	22.63	98.23	21.42	21.8
LCSF30-1	56.23	14.75	26.23	113.65	9.6	8.44	163.25	35.75	21.9
LCSF36-0.5	42.57	27.07	63.59	106.77	12.4	11.61	158.18	6.07	3.83
LCSF36-1	38.95	18.13	46.55	107.23	13.47	12.56	178.11	23.73	13.32
LCSF60-0.5	46.31	14.38	31.06	102.02	17.49	17.14	150.26	29.39	19.52
LCSF60-1	78.51	3.42	4.35	129.21	64.21	49.69	211.98	63.51	29.96

Results for G-BCN test for all mixtures are presented at Table 4.11. Average values, standard deviation and coefficient of variation values are presented at Table 4.12. LCSF30-0.5 and LCSF30-1 have high of coefficient of variation. Although both values are still lower than maximum coefficient of variation value (24%) for 3 point bending test, considering the dispersion in the results of Barcelona test values as well, it is possible to say that Barcelona test does not provide significant improvement on the scattering of results in general. This finding is not parallel with the arguments presented at Carmona *et al.* [48].

Plain concrete LC failed immediately at the peak load without any ductile behavior. Considering 0.5% volume fraction fibers LCSF36 has the highest toughness at 3.5mm axial displacement. For 1% volume fraction LCSF60-1 has the highest toughness at 3.5mm axial displacement as it is expected. It can be noted that very low fraction of fibers (0.5%) does not consistently represent the expected behavior of concrete. Whereas with volume fraction of 1% and above may result more dramatic improvement in ductile behavior. Average toughness values for different axial displacements presented at Figure 4.10.

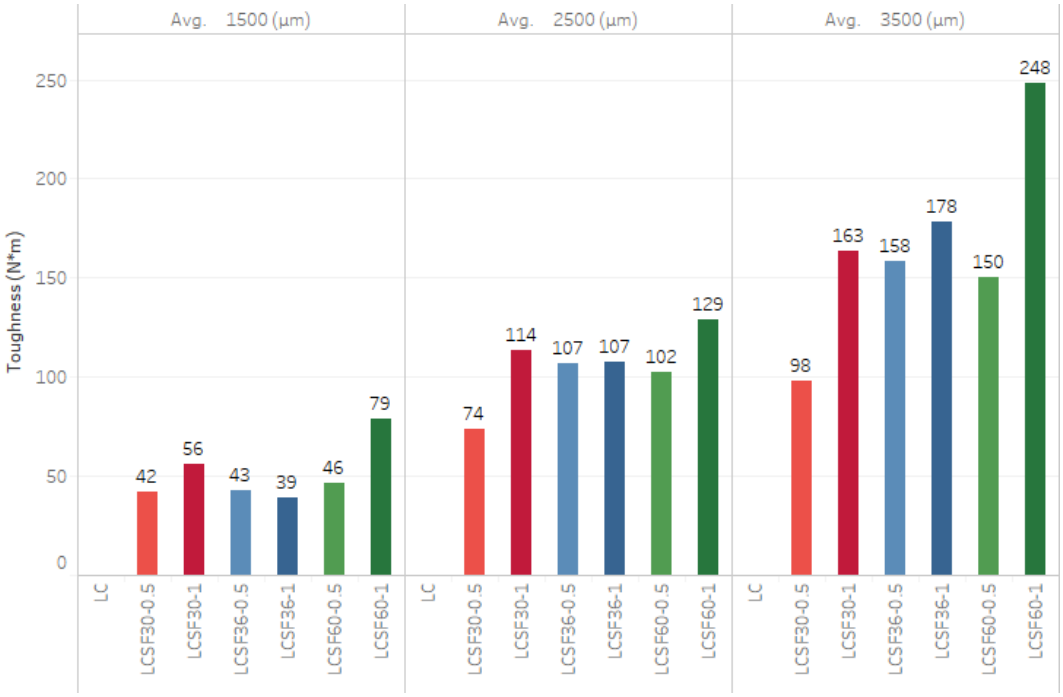

Figure 4.9. Average G-BCN toughness values (N*m)

5. CONCLUSIONS

This study included production of pumice lightweight aggregate steel fiber reinforced concrete with three different aspect ratios and two different volume fraction of steel fibers. Here are the observations according to the results of the current study:

- The workability of concrete decrease significantly by the addition of fibers. In order to compensate this effect, different amounts of superplasticizers were used.
- Addition of steel fibers increased unit weight of concrete. Yet replacement of pumice kept all the specimens in the limits of lightweight-aggregate concrete density.
- Capping decreased the compressive strength values by 40%. Sanding the top of some specimens was needed.
- Addition of fibers has inconsistent effects on compressive strength.
- There is no significant effect on modulus of elasticity by the addition of fibers.
- Increasing volume fraction of fibers from 0.5% to 1% does not affect modulus of elasticity.
- There is no significant effect on Poisson's ratio by the addition of steel fibers.
- f_{LOP} values are increasing as the fiber aspect ratio and volume fraction tend to increase.
- Addition of fibers has significant positive effect on flexural strength (modulus of rupture) of the specimens.
- Only LCSF30 specimens with both volume fractions of 0.5% and 1% have softening behavior. With all the other specimens with fibers, hardening behavior is observed.
- Toughness and Fracture Energy parameters are increased significantly with increasing fiber aspect ratio and volume fraction of fibers. Ductility of specimens are also improved with the same manner.

- Indirect tensile strength does not improve significantly with the addition of fibers. Better improvement would be observed with higher volume fraction of fibers. (>1%)
- Barcelona and Generalized Barcelona tests do not necessarily have lesser scattering (or coefficient of variation) than 3 point bending test results.
- Barcelona and Generalized Barcelona tests are faster, lighter and more environmentally friendly tests than other fracture tests.

REFERENCES

1. Palucka, Tim, and Bernadette Bensaude-Vincent, “Composites overview”, *History of Recent Science and Technology.–19 жовтня* (2002).

2. Jones, Robert M., *Mechanics of Composite Materials*, CRC press, 2014.

3. Ashby, Michael F., and D. Cebon. "Materials selection in mechanical design." *Le Journal de Physique IV* 3.C7 (1993): C7-1.

4. Hull, Derek, and Trevor W. Clyne., *An introduction to composite materials*, Cambridge university press, 1996.

5. Barbero, Ever J., *Introduction to Composite Materials Design*, CRC press, 2017.

6. Peters, Stanley T., ed. *Handbook of composites*. Springer Science & Business Media, 2013.

7. D.B. Miracle and S.L. Donaldson, *ASM Handbook of Composites*, Volume 21, (2001)

8. Bentur, Arnon, and Sidney Mindess., *Fibre reinforced cementitious composites*, CRC Press, 2014.

9. Naaman, Antoine E. "Fiber reinforced concrete: State of progress at the edge of the new millennium." *Design and Sustainability* (2007)

10. *Report on Fiber Reinforced Concrete*, ACI 544.2R-89

11. ASTM A820 / A820M-16, *Standard Specification for Steel Fibers for Fiber-Reinforced Concrete*, ASTM International, West Conshohocken, PA, 2016.

12. Edgington, J., and D. J. Hannant. "Steel fibre reinforced concrete. The effect on fibre orientation of compaction by vibration." *Matériaux et Construction* 5.1 (1972): 41-44.

13. Kang, Su Tae, *et al.*, "The effect of fibre distribution characteristics on the flexural strength of steel fibre-reinforced ultra high strength concrete.", *Construction and Building Materials*, 25.5 (2011): 2450-2457.

14. Aveston, J., "Fibre reinforced cements-scientific foundations for specifications." National Physical Laboratory Conference Proceedings, Composite-Standards testing and design, 1974.

15. Laws, V., "The efficiency of fibrous reinforcement of brittle matrices.", *Journal of Physics D: Applied Physics*, 4.11 (1971): 1737.

16. Allen, H. G. "The strength of thin composites of finite width, with brittle matrices and random discontinuous reinforcing fibres." *Journal of Physics D: Applied Physics* 5.2 (1972): 331.

17. Alberti, M. G., A. Enfedaque, and J. C. Gálvez. "On the prediction of the orientation factor and fibre distribution of steel and macro-synthetic fibres for fibre-reinforced concrete." *Cement and Concrete Composites* 77 (2017): 29-48.

18. Abrishambaf, Amin, Mário Pimentel, and Sandra Nunes. "Influence of fibre orientation on the tensile behaviour of ultra-high performance fibre reinforced cementitious composites." *Cement and Concrete Research* 97 (2017): 28-40.

19. Johnston, Colin D. Fiber-reinforced cements and concretes. Crc Press, 2014.

20. Mehdipour, Iman, *et al.*, "Effect of workability characteristics on the hardened performance of FRSCCMs.", *Construction and Building Materials*, 40 (2013): 611-621.

21. Hassanpour, Mahmoud, Payam Shafigh, and Hilmi Bin Mahmud. "Lightweight aggregate concrete fiber reinforcement–a review.", *Construction and Building Materials*, 37 (2012): 452-461.

22. Satish, Chandra, and L. Berntsson., "Lightweight aggregate concrete, science, technology, and applications.", *Published in the USA by Noyes Publications/William Andrew Publishing*, 2002.

23. Balendran, R. V., *et al.* "Influence of steel fibres on strength and ductility of normal and lightweight high strength concrete." *Building and environment* 37.12 (2002): 1361-1367.

24. Choi, Jisun, *et al.*, "Influence of fiber reinforcement on strength and toughness of all-lightweight concrete." *Construction and Building Materials* 69 (2014): 381-389.

25. Zhang, Min Hong, and Odd E. Gjvorv, "Mechanical properties of high-strength lightweight concrete.", *Materials Journal* 88.3 (1991): 240-247.

26. Bayasi, M. Ziad, and Parviz Soroushian, "Effect of steel fiber reinforcement on fresh mix properties of concrete.", *Materials Journal* 89.4 (1992): 369-374.

27. Chu, S. H., L. G. Li, and A. K. H. Kwan, "Fibre factors governing the fresh and hardened properties of steel FRC.", *Construction and Building Materials*, 186 (2018): 1228-1238.

28. Abbass, Wasim, M. Iqbal Khan, and Shehab Mourad, "Evaluation of mechanical properties of steel fiber reinforced concrete with different strengths of concrete.", *Construction and Building Materials*, 168 (2018): 556-569.

29. Song, P. S., and S. Hwang, "Mechanical properties of high-strength steel fiber-reinforced concrete.", *Construction and Building Materials*, 18.9 (2004): 669-673.

30. Iqbal, Shahid, *et al.*, "Mechanical properties of steel fiber reinforced high strength lightweight self-compacting concrete (SHLSCC).", *Construction and Building Materials*, 98 (2015): 325-333.

31. Kim, Yong Jic, Yun Wang Choi, and Mohamed Lachemi, "Characteristics of self-consolidating concrete using two types of lightweight coarse aggregates.", *Construction and Building Materials*, 24.1 (2010): 11-16.

32. Lo, T. Y., *et al.*, "Comparison of workability and mechanical properties of self-compacting lightweight concrete and normal self-compacting concrete.", *Materials Research Innovations*, 11.1 (2007): 45-50.

33. Shafigh, Payam, *et al.*, "A comparison study of the fresh and hardened properties of normal weight and lightweight aggregate concretes.", *Journal of building Engineering*, 15 (2018): 252-260.

34. Kockal, Niyazi Ugur, and Turan Ozturan., "Strength and elastic properties of structural lightweight concretes.", *Materials & Design*, 32.4 (2011): 2396-2403.

35. Campione, G., N. Miraglia, and M. Papia, "Mechanical properties of steel fibre reinforced lightweight concrete with pumice stone or expanded clay aggregates.", *Materials and Structures*, 34.4 (2001): 201-210.

36. Düzgün, Oğuz Akın, Rüstem Gül, and Abdulkadir Cüneyt Aydi,. "Effect of steel fibers on the mechanical properties of natural lightweight aggregate concrete.", *Materials Letters*, 59.27 (2005): 3357-3363.

37. Libre, Nicolas Ali, *et al.*, "Mechanical properties of hybrid fiber reinforced lightweight aggregate concrete made with natural pumice.", *Construction and Building Materials*, 25.5 (2011): 2458-2464.

38. ASTM D75 / D75M-14, Standard Practice for Sampling Aggregates, ASTM International, West Conshohocken, PA, 2014.

39. ASTM C136 / C136M-14, Standard Test Method for Sieve Analysis of Fine and Coarse Aggregates, ASTM International, West Conshohocken, PA, 2014.

40. Fuller, William B., and Sanford E. Thompson, "The laws of proportioning concrete.", (1907): 67-143.

41. ASTM C192 / C192M-16a, Standard Practice for Making and Curing Concrete Test Specimens in the Laboratory, ASTM International, West Conshohocken, PA, 2016.

42. ASTM C143 / C143M-15a, Standard Test Method for Slump of Hydraulic-Cement Concrete, ASTM International, West Conshohocken, PA, 2015.

43. ASTM C138 / C138M-17a, Standard Test Method for Density (Unit Weight), Yield, and Air Content (Gravimetric) of Concrete, ASTM International, West Conshohocken, PA, 2017.

44. ASTM C39 / C39M-18, Standard Test Method for Compressive Strength of Cylindrical Concrete Specimens, ASTM International, West Conshohocken, PA, 2018.

45. ASTM C469-02, Standard Test Method for Static Modulus of Elasticity and Poisson's Ratio of Concrete in Compression, ASTM International, West Conshohocken, PA, 2002.

46. BS EN 14651 + A1:2007, Test method for metallic fibered concrete - Measuring the flexural tensile strength (limit of proportionality (LOP), residual), European Standard, June (2005)

47. UNE 83-515:2008. Hormigones con fibras. Determinación de la resistencia a fisuración, tenacidad y resistencia residual a tracción. Método Barcelona (in Spanish)

48. Carmona, Sergio, Antonio Aguado, and Climent Molins, "Characterization of the properties of steel fiber reinforced concrete by means of the generalized Barcelona test.", *Construction and Building Materials*, 48 (2013): 592-600.

APPENDIX A: LOAD-CMOD CURVES FOR 3 POINT BENDING TEST

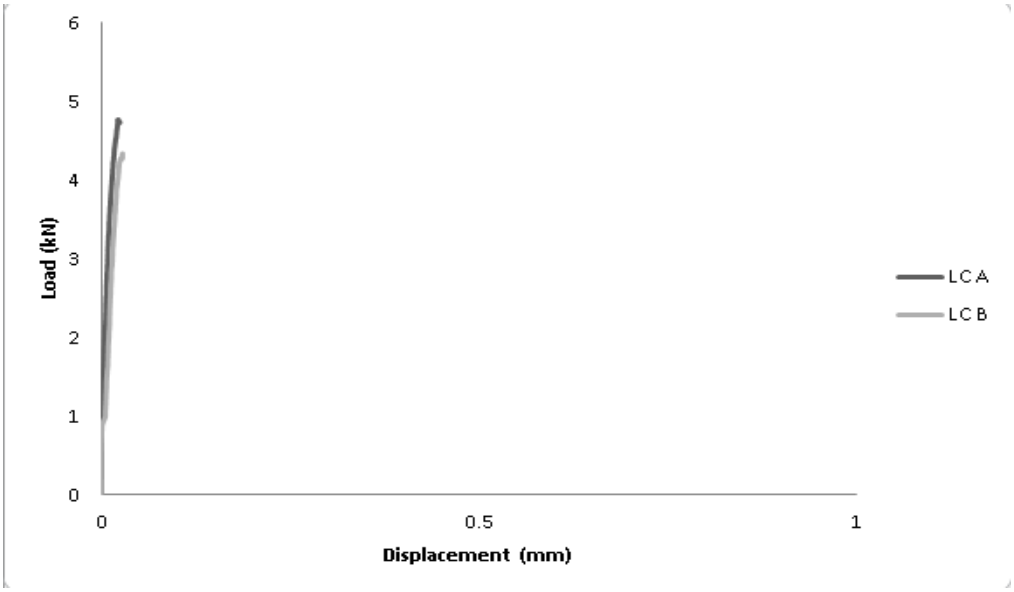

Figure A.1. Load-CMOD curves of LC specimens in 3 point bending test

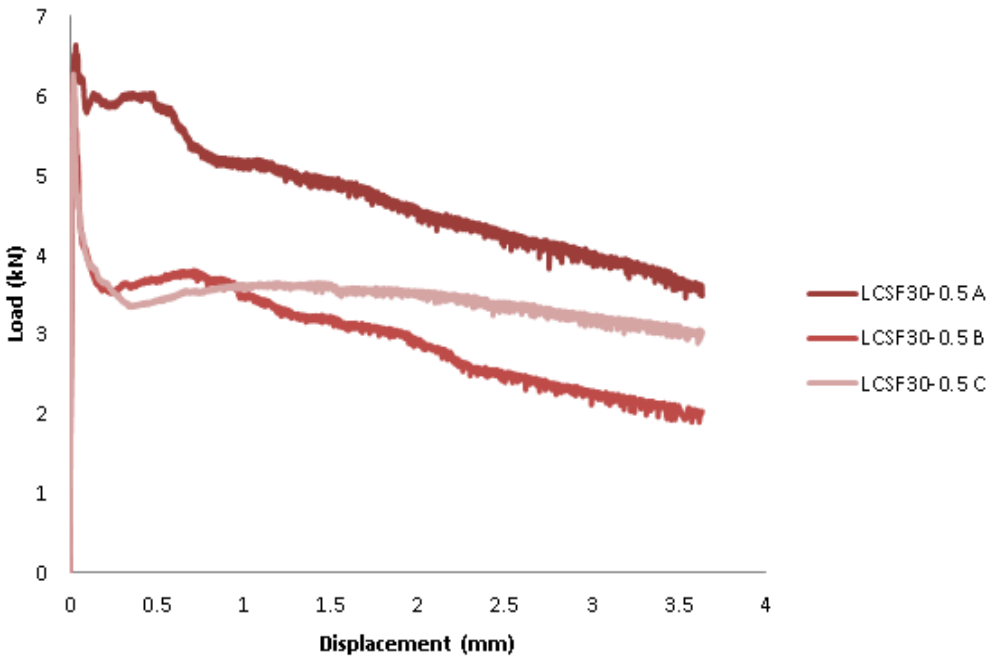

Figure A.2. Load-CMOD curves of LCSF30-0.5 specimens in 3 point bending test

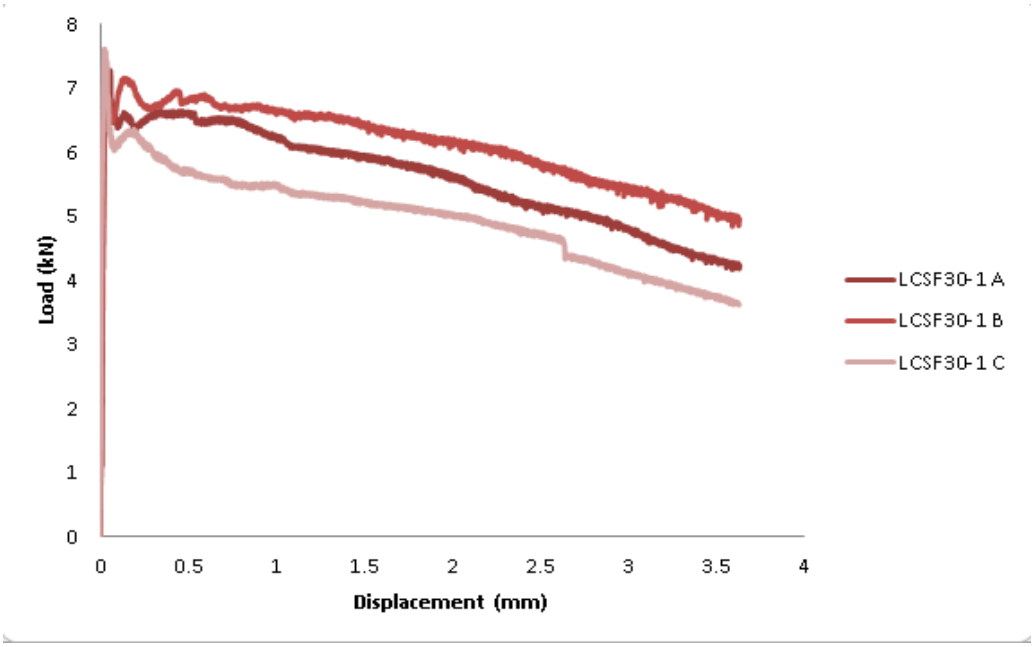

Figure A.3. Load-CMOD curves of LCSF30-1 specimens in 3 point bending test

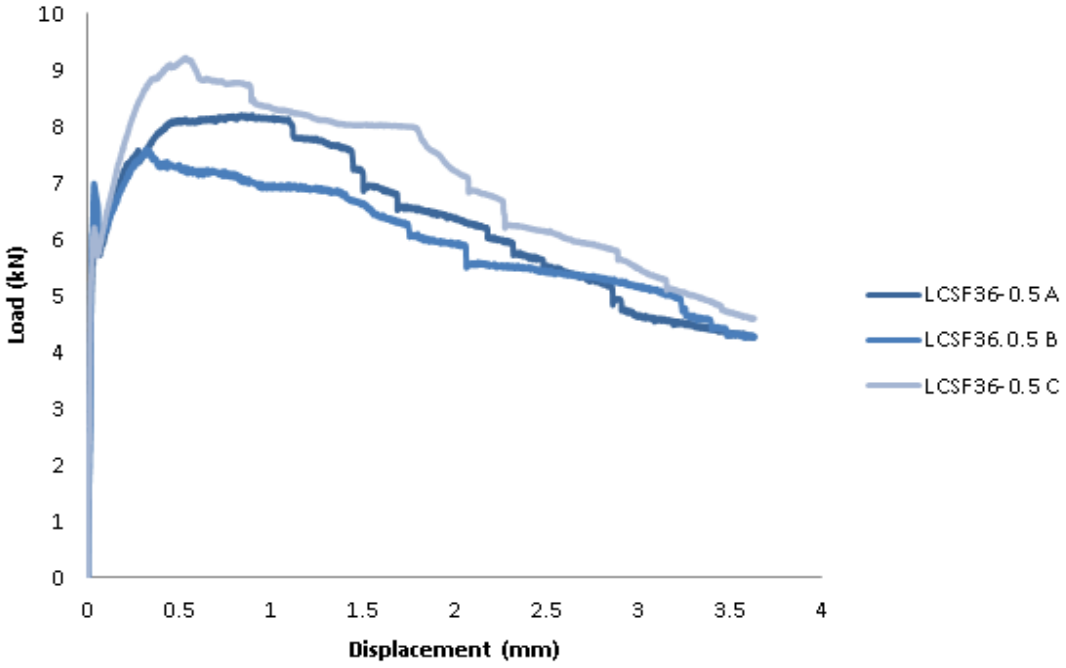

Figure A.4. Load-CMOD curves of LCSF36-0.5 specimens in 3 point bending test

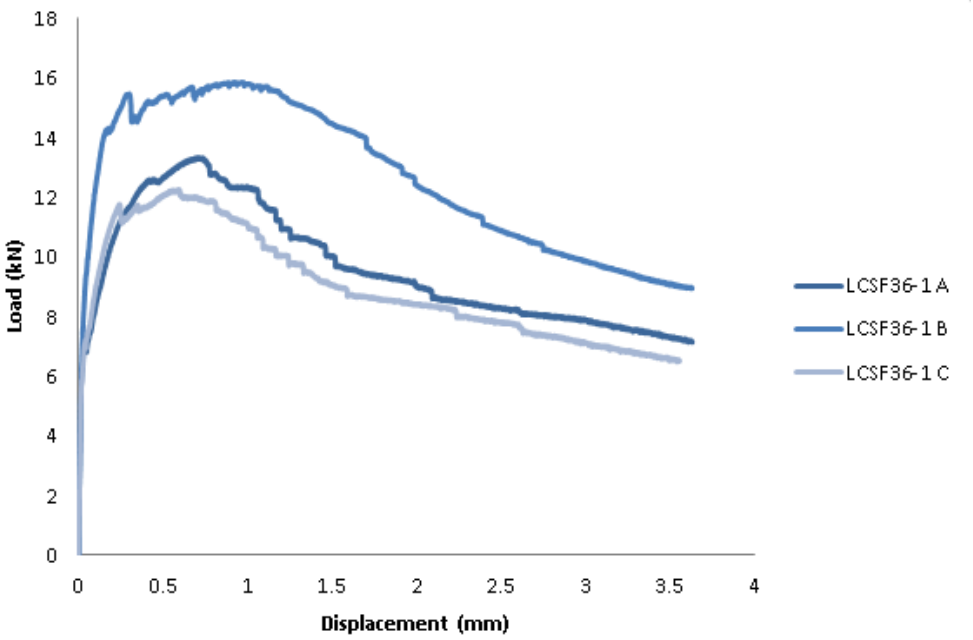

Figure A.5. Load-CMOD curves of LCSF36-1 specimens in 3 point bending test

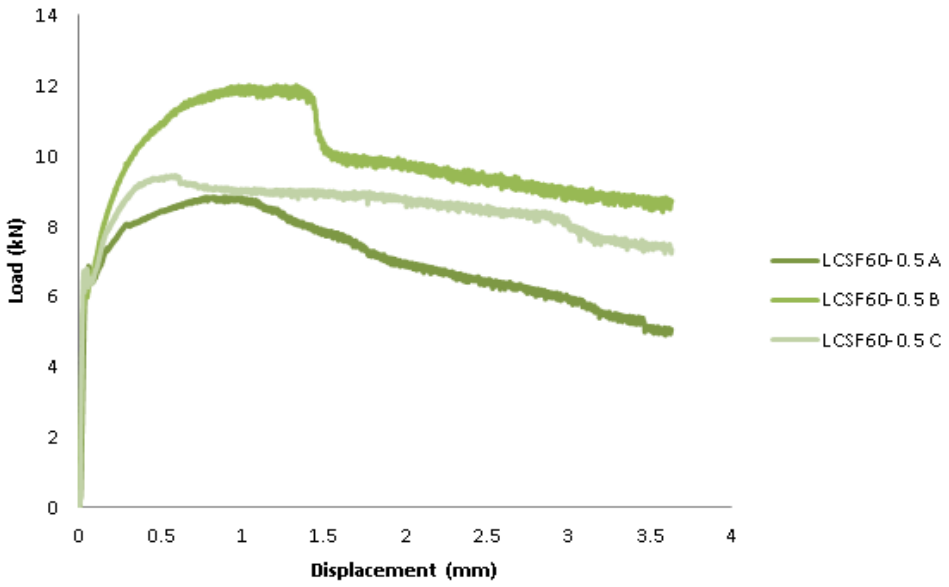

Figure A.6. Load-CMOD curves of LCSF60-0.5 specimens in 3 point bending test

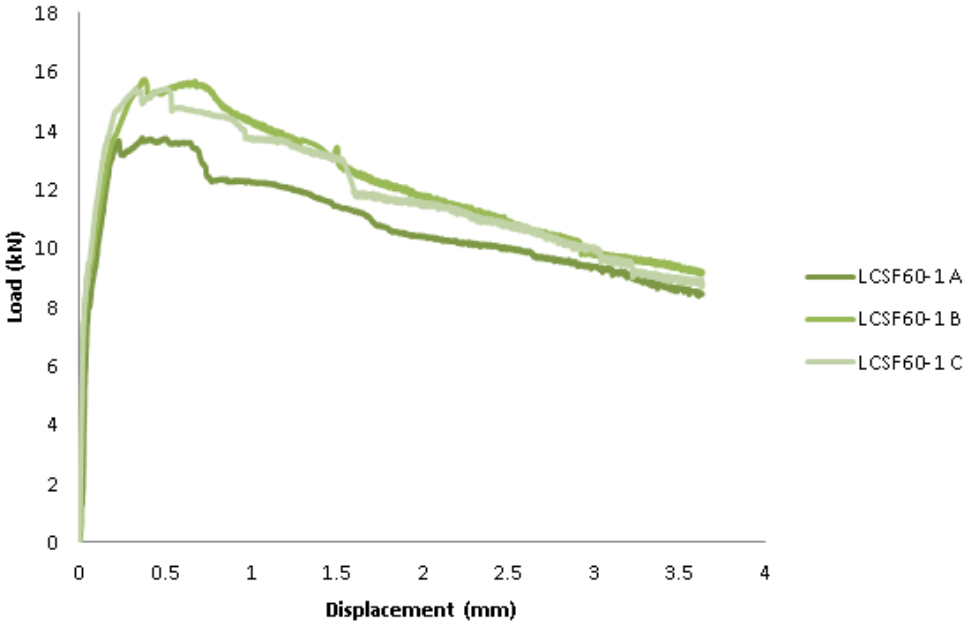

Figure A.7. Load-CMOD curves of LCSF60-1 specimens in 3 point bending test

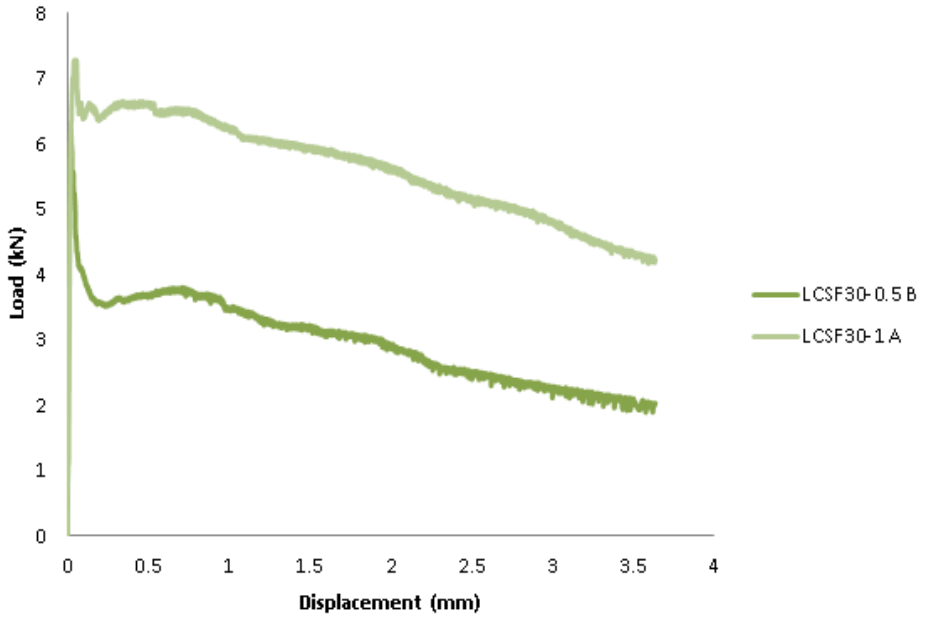

Figure A.8. Load-CMOD curves of different volume fractions of fibers for LCSF30 series (Average behaviors are taken)

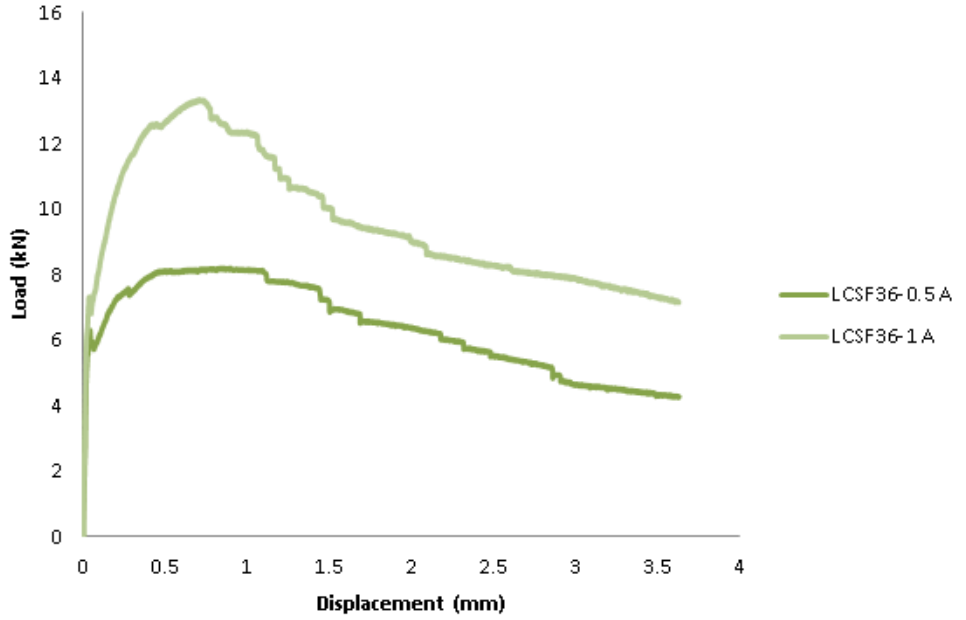

Figure A.9. Load-CMOD curves of different volume fractions of fibers for LCSF60 series (Average behaviors are taken)

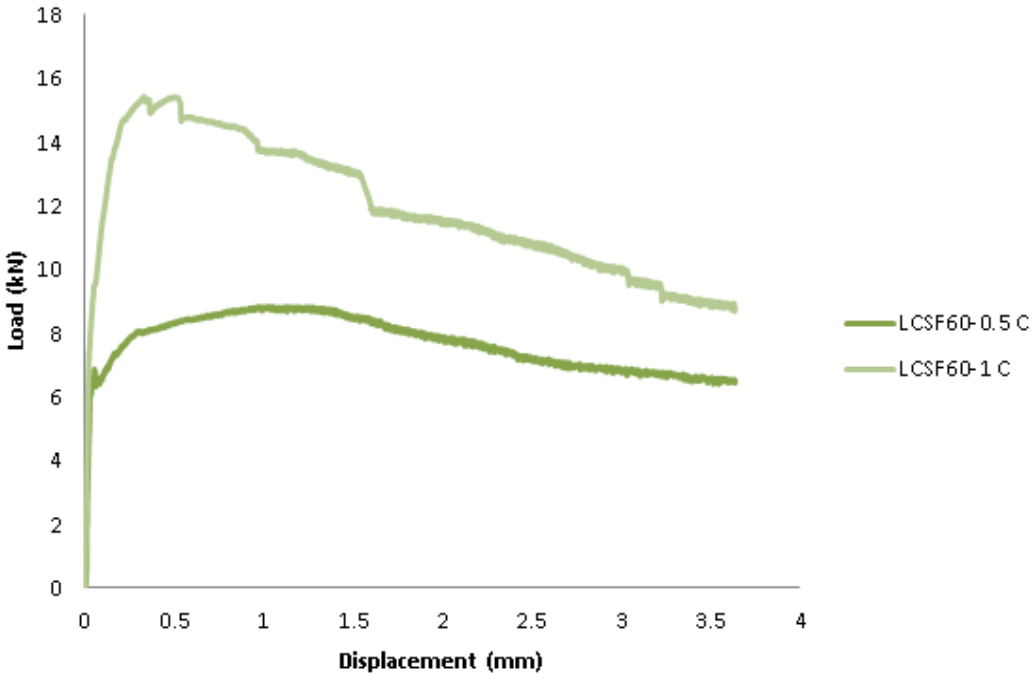

Figure A.10. Load-CMOD curves of different volume fractions of fibers for LCSF60 series (Average behaviors are taken)

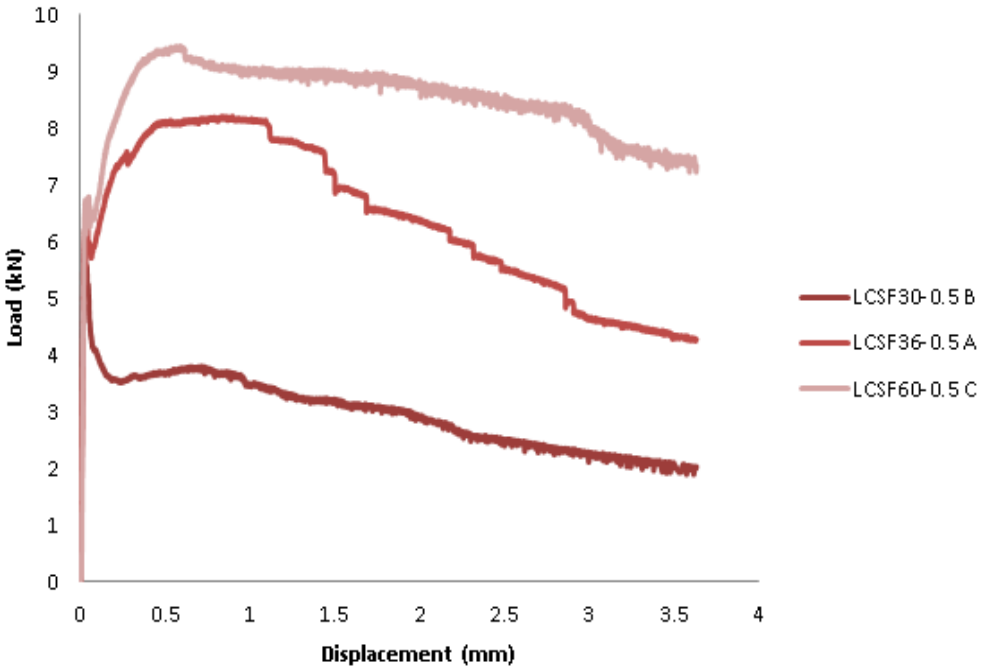

Figure A.11. Load-CMOD curves of different fiber length for 0.5% fibers (Average behaviors are taken)

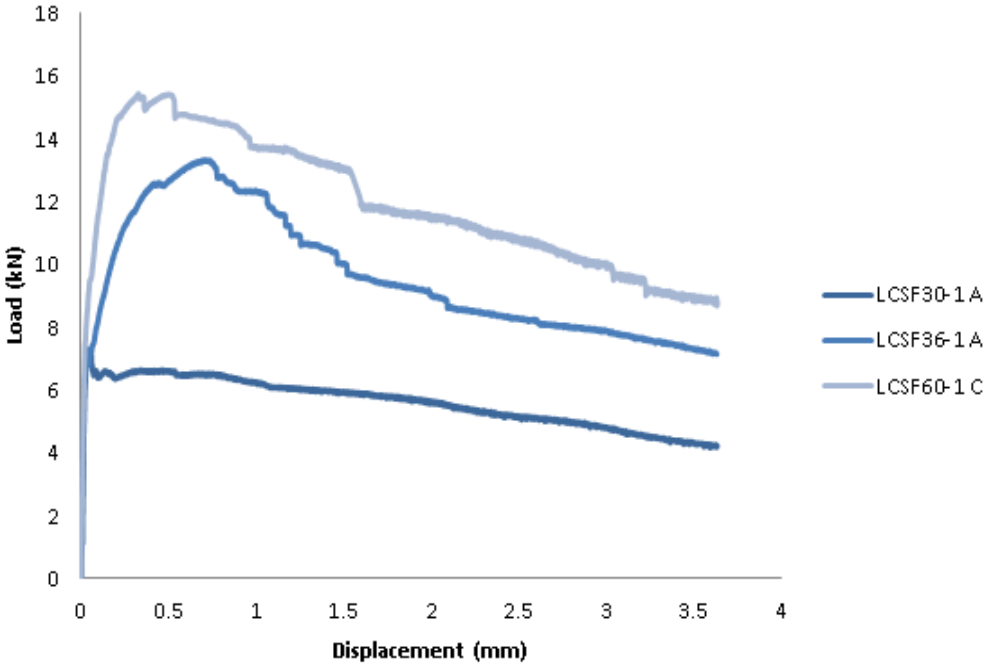

Figure A.12. Load-CMOD curves of different fiber length for 1% fibers (Average behaviors are taken)